AD-A114 546 CALIFORNIA RESEARCH AND TECHNOLOGY INC WOODLAND HILLS F/G 18/3
INTRODUCTION TO NUCLEAR DUST/DEBRIS CLOUD FORMATION.(U)
JUL 81 M ROSENBLATT DNA001-80-C-0018
UNCLASSIFIED CRT-3370 DNA-5832T NL

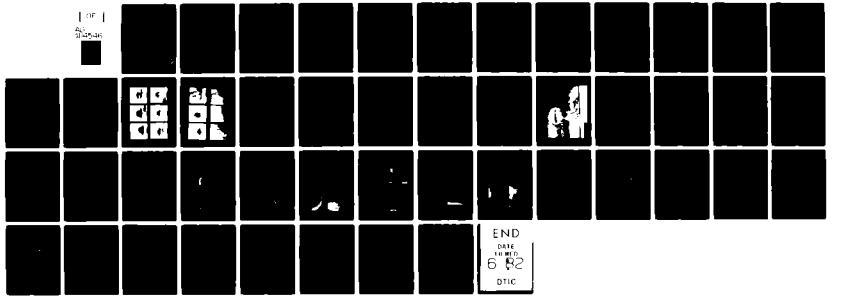

(12)

DNA 5832T

INTRODUCTION TO NUCLEAR DUST/DEBRIS CLOUD FORMATION

Martin Rosenblatt
California Research and Technology, Inc.
6269 Variel Avenue
Woodland Hills, California 91367

1 July 1981

Topical Report for Period 7 November 1979—1 July 1981

CONTRACT No. DNA 001-80-C-0018

APPROVED FOR PUBLIC RELEASE;
DISTRIBUTION UNLIMITED.

THIS WORK SPONSORED BY THE DEFENSE NUCLEAR AGENCY
UNDER RDT&E RMSS CODE B342080464 N99QAXAG12815 H2590D.

Prepared for
Director
DEFENSE NUCLEAR AGENCY
Washington, D. C. 20305

Destroy this report when it is no longer needed. Do not return to sender.

PLEASE NOTIFY THE DEFENSE NUCLEAR AGENCY, ATTN: STTI, WASHINGTON, D.C. 20305, IF YOUR ADDRESS IS INCORRECT, IF YOU WISH TO BE DELETED FROM THE DISTRIBUTION LIST, OR IF THE ADDRESSEE IS NO LONGER EMPLOYED BY YOUR ORGANIZATION.

UNCLASSIFIED

SECURITY CLASSIFICATION OF THIS PAGE (When Data Entered)

REPORT DOCUMENTATION PAGE		READ INSTRUCTIONS BEFORE COMPLETING FORM
1. REPORT NUMBER DNA 5832T	2. GOVT ACCESSION NO AD-A114 546	3. RECIPIENT'S CATALOG NUMBER
4. TITLE (and Subtitle) INTRODUCTION TO NUCLEAR DUST/DEBRIS CLOUD FORMATION		5. TYPE OF REPORT & PERIOD COVERED Topical Report for Period 7 Nov 79—1 Jul 81
		6. PERFORMING ORG. REPORT NUMBER CRT 3370
7. AUTHOR(s) Martin Rosenblatt		8. CONTRACT OR GRANT NUMBER(s) DNA 001-80-C-0018
9. PERFORMING ORGANIZATION NAME AND ADDRESS California Research & Technology, Inc. 6269 Variel Avenue Woodland Hills, California 91367		10. PROGRAM ELEMENT, PROJECT, TASK AREA & WORK UNIT NUMBERS Subtask N99QAXAG128-15
11. CONTROLLING OFFICE NAME AND ADDRESS Director Defense Nuclear Agency Washington, D.C. 20305		12. REPORT DATE 1 July 1981
		13. NUMBER OF PAGES 48
14. MONITORING AGENCY NAME & ADDRESS(if different from Controlling Office)		15. SECURITY CLASS. (of this report) UNCLASSIFIED
		15a. DECLASSIFICATION/DOWNGRADING SCHEDULE N/A

16. DISTRIBUTION STATEMENT (of this Report)

Approved for public release; distribution unlimited.

17. DISTRIBUTION STATEMENT (of the abstract entered in Block 20, if different from Report)

18. SUPPLEMENTARY NOTES

This work sponsored by the Defense Nuclear Agency under RDT&E RMSS Code B342080464 N99QAXAG12815 H2590D.

19. KEY WORDS (Continue on reverse side if necessary and identify by block number)

Nuclear Clouds	Debris
Dust	Sweep-Up Layer
Ejecta	Dust Pedestal

20. ABSTRACT (Continue on reverse side if necessary and identify by block number)

The detonation of a nuclear device on or near the Earth's surface generates a lofted cloud composed of dust and other debris. The objectives of this report are to provide (1) an overview of dust/debris cloud phenomenology and (2) examples of cloud characteristics. Physical phenomenology associated with surface bursts (e.g., crater ejecta) and airbursts (e.g., shock reflections and sweep-up layer formation) are discussed and examples are presented.

DD FORM 1 JAN 73 1473 EDITION OF 1 NOV 65 IS OBSOLETE

UNCLASSIFIED

SECURITY CLASSIFICATION OF THIS PAGE (When Data Entered)

PREFACE

Questions concerning dust/debris environments generated by surface and near-surface nuclear detonations continue to be asked by defense planners. This report is intended to introduce the subject to those individuals not familiar with nuclear dust/debris cloud formation.

Lt. Col. R. E. Case (DNA/SPAS) was the technical monitor for this work and his helpful suggestions are gratefully acknowledged.

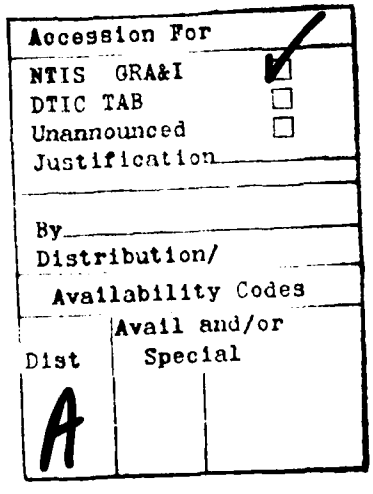

Table of Conversion Factors
for Units Used in This Report

Physical Quantity	To convert from units in report	To metric (SI) units	Multiply by
Mass	pound	kilogram (kg)	.454
	ton	kilogram (kg)	10^3
	kton	kilogram (kg)	10^6
Energy	ton	joules (J)	4.2×10^9
	kton	joules (J)	4.2×10^{12}
	Mton	joules (J)	4.2×10^{15}
Pressure	bar*	pascal (Pa)	10^5
	psi*	pascal (Pa)	6895.
Density	gm/cm^3	kg/m^3	10^3
Length	foot	meter (m)	.3048

*1 bar = 14.5 psi
1 psi = .06895 bar

TABLE OF CONTENTS

LIST OF ILLUSTRATIONS

LIST OF ILLUSTRATIONS (continued)

LIST OF ILLUSTRATIONS (continued)

SECTION 1

INTRODUCTION

1.1 BACKGROUND AND OBJECTIVES

The detonation of one or more nuclear weapons on or near the Earth's surface generate a lofted cloud composed of dust and other debris.

The lofted mass is a potential threat to

- *reentry vehicles* which must fly through clouds from prior detonations (fratricide)
- *ascent vehicles* which must flyout soon after being attacked
- *radar* and *communications* which must operate in a dust/debris environment

The objectives of this report are to provide interested persons with

1. an overview of dust/debris cloud phenomenology
2. examples of cloud characteristics

1.2 BASIC CONCEPTS

After a near-surface nuclear burst, the cloud characteristics of primary interest are the concentration* and particle size distribution of the condensed phase mass in the cloud as a function of position and time.

The condensed phase mass in the cloud can be composed of:

- *earth material* which has been entrained and lofted by the ascending winds which develop. (Earth or ground material include soil/rock, water, vegetation, as well as structures near the burst point.)
- *weapon material* which has been vaporized and recondenses during the early phases of the nuclear cloud development.
- *water/ice* particles which condense from relatively moist (humid) air which is entrained and lofted from near the Earth's surface to higher and colder regions of the atmosphere.

Particle is a generic term which includes dust, pebbles, rocks, boulders, water, ice, or any other condensed phase mass in the cloud. The lofted particles are of many different sizes and shapes. For convenience, the size of a particle is usually taken as the equivalent spherical diameter, a:

$$a \equiv \left(\frac{6m}{\rho_o \pi}\right)^{1/3}$$

Diameter (m = 1 gm when a = 1 cm and ρ_o = 1.9 gm/cm^3)

where

m	Mass of particle
ρ_o	Density of particle

*Mass concentration is also commonly called density.

The weapon yield (W) is the energy released in a nuclear detonation.* The yield is usually expressed in equivalent tons of TNT, where

1 ton of TNT is assumed to release 10^9 calories or 4.2×10^3 Joules

1 kiloton = 1 kt = 4.2×10^{12} Joules

1 megaton = 1 Mt = 4.2×10^{15} Joules

The first nuclear detonation, shot TRINITY in 1945, had a yield of ~19 kt. The yields of the weapons detonated over Hiroshima and Nagasaki were approximately 13 kt and 23 kt, respectively. Shot CASTLE BRAVO in 1954 at Bikini (in the Pacific Proving Ground) had the largest U.S. test yield of ~15 Mt.

The height of burst (HOB) is the device height above the Earth's surface. The scaled height of burst (SHOB) is defined as

$$SHOB = HOB/W^{1/3} \qquad (2\text{-}1)$$

Buried bursts have negative HOB and SHOB.

A contact surface burst is defined as $|SHOB| < 5$ ft/kt$^{1/3}$. A nuclear detonation this close to the ground surface causes a dynamic cratering process which ejects large amounts of earth material into the atmosphere. A contact surface burst couples about 8% of the nuclear yield to the ground in a few microseconds. The details of the energy coupled to the ground, and the amount of ejecta thrown into the atmosphere will depend on W, HOB, the device construction, and the properties of the ground material.

---

*The nature of the nuclear energy released and a general description of nuclear weapons effects are in Reference 1.

As the SHOB increases above 5 ft/kt$^{1/3}$ (i.e., about 50 ft for W = 1 megaton), the fraction of energy coupled directly to the ground and the amount of ejected mass begins to decrease rapidly. An estimate of the crater ejecta mass source vs HOB and SHOB for W = 1 megaton is shown in Figure 1 below. All other sources of ground material which become entrained in the nuclear cloud come from near the ground surface and can be conveniently combined into the sweep-up mass source. The sweep-up mass source dominates the lofted cloud mass characteristics for SHOB $\gtrsim$ 20 ft/kt$^{1/3}$.

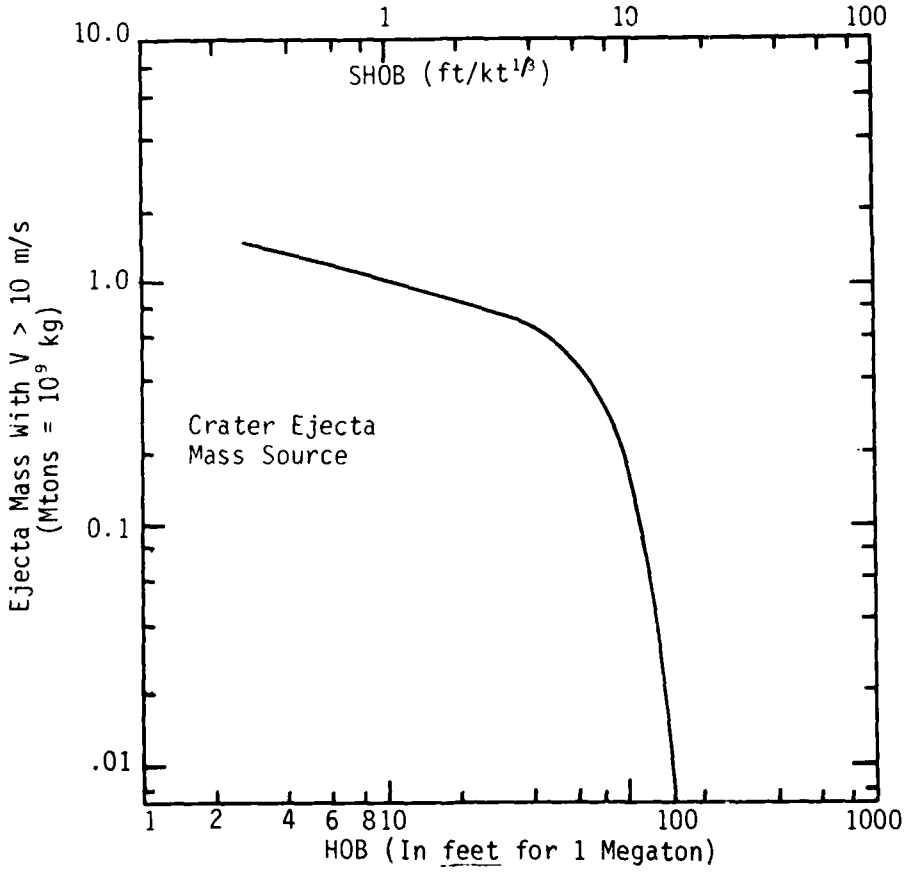

Fig. 1. Crater Ejecta Mass Source with Ejection Speeds of Over 10 m/s versus HOB for W = 1 Mt.[2]

SECTION 2

DUST/DEBRIS SOURCES

2.1 CRATER EJECTA MASS SOURCE

For contact surface bursts, crater ejecta represents the primary source of ground material which becomes entrained in the nuclear cloud. The following figure indicates the general physical phenomena, pressures, and times involved in crater formation for a nominal 1 megaton contact surface detonation.

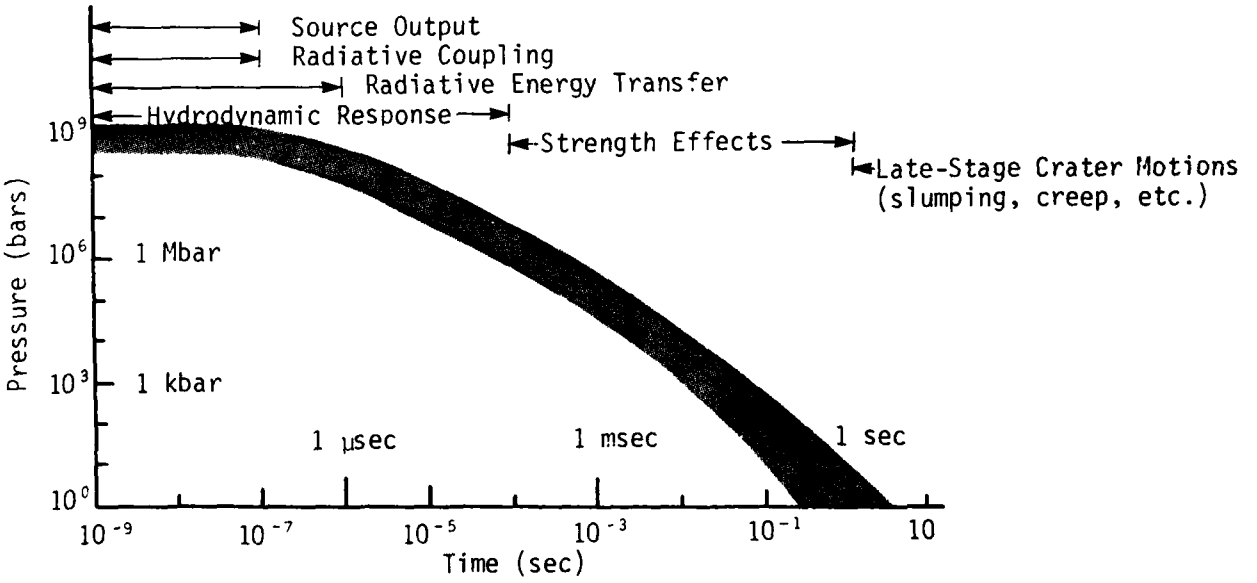

Fig. 2. Typical Pressure-Time Sequence for Energy Coupling and Cratering.[3]

The following photos show the fireball and ejecta from the slightly buried burst JOHNIE BOY (W = 0.5 kt, HOB ~-2.0 ft, at NTS). Note that some of the crater ejecta emerges from the early-time fireball in distinct rays.

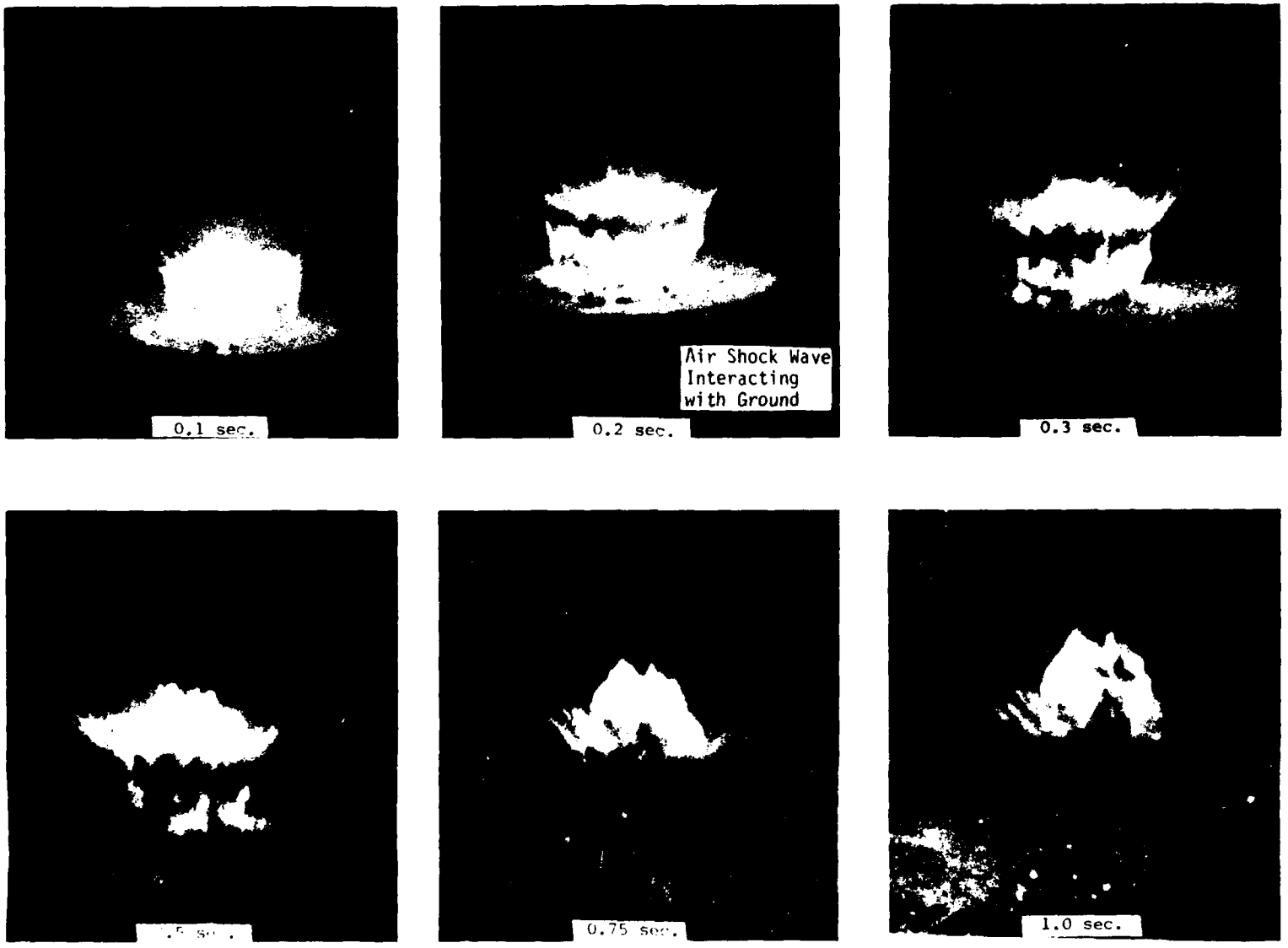

Fig. 3. Photographic Example for Shot JOHNIE BOY (W = 0.5 kt, DOB = .6 m).[4]

PLATE 14

HORIZONTAL SCALE 5.7 meters/mm

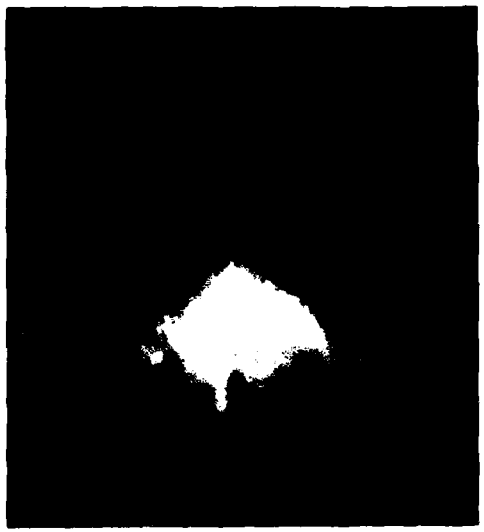

0.8 sec.

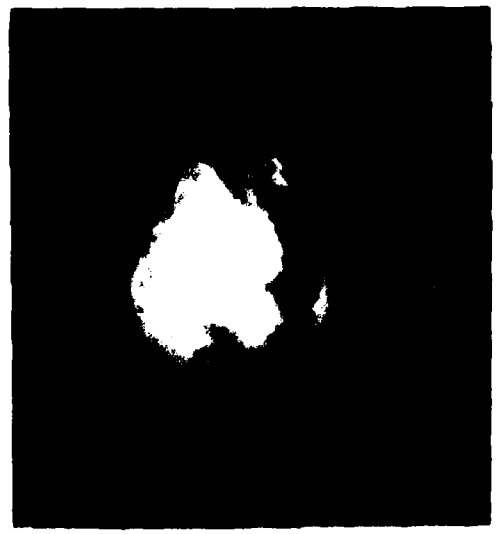

2.0 sec.

4.0 sec.

SCALE (.8-4 sec.) 4.5 meters/mm

8.0 sec.

12. sec.

20. sec.

SCALE (8-20 sec.) 8.5 meters/mm

Fig. 4. Photographic Example for Shot JOHNIE BOY (W = 0.5 kt, DOB = .6 m).[4]

PLATE 15

Theoretical calculations (or computer code simulations) of the crater and ejecta formation use finite difference analogues of the differential equations for conservation of mass, conservation of momenta, conservation of energy, and approximate equations of state for the weapon and ground materials.

These numerical simulations predict the particle velocity, density and temperature of the incipient ejecta versus radius and time. (Most crater/ejecta calculations are axisymmetric and ejecta rays are ignored.) Figure 5 (next page) shows a velocity vector field near the dynamic crater at t ~0.2 seconds for a 1 Mt contact burst over the indicated geology. The incipient ejecta is flowing through the original ground surface (Z = 0) at radii between 40 m and 80 m at 0.2 seconds. The ejection angles are roughly 45°.

The ejecta mass rate per unit area flowing across Z = 0 at any radius is ρV. At t = 0.2 seconds, ρV peaks at a radius of about 50 meters and has an associated vertical velocity of ~60 m/s. Figure 6 shows the analogous vertical velocity (i.e., associated with the peak mass flux) as a function of time from 5 nuclear cratering calculations. The various calculations show variations of about a factor of 2 from the mean curve.

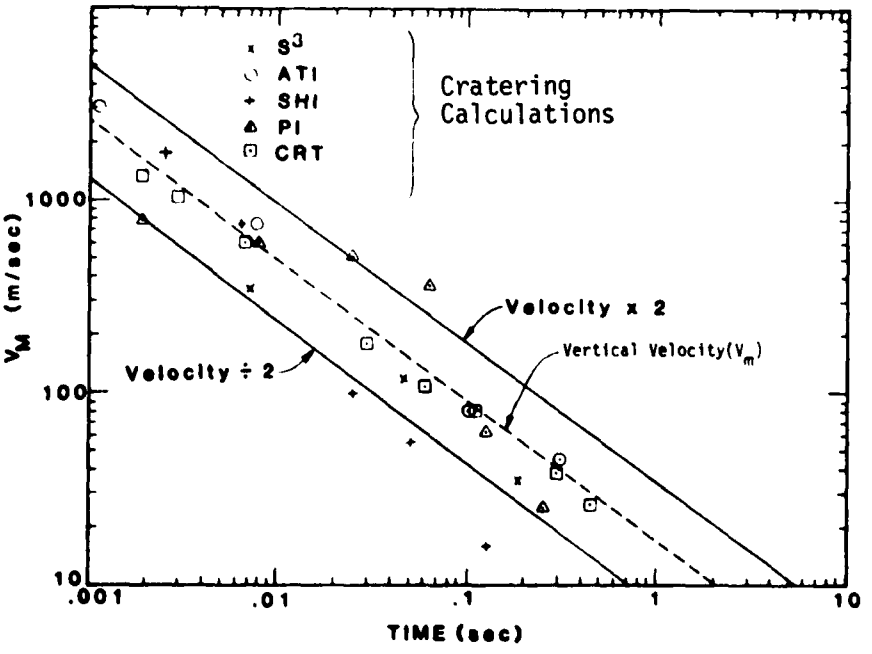

Fig. 6. Ejecta Vertical Velocity at a Range of Greatest Mass Flux from Cratering Calculations for a 1 Mt Surface Burst.[5,6]

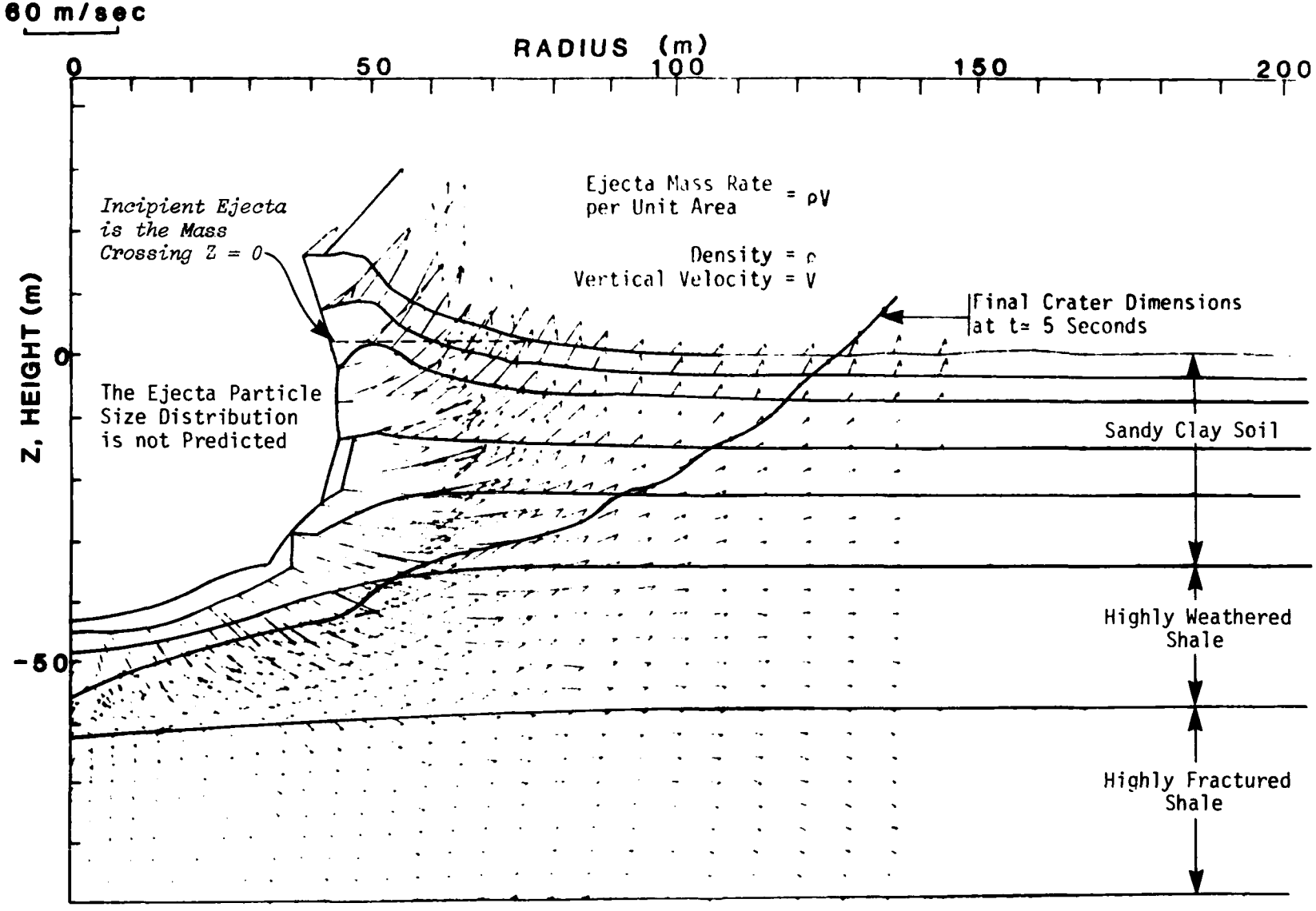

Fig. 5. Crater Ejecta Source Example: Velocity Field at t ~0.2 Seconds for a W = 1 Mt Surface Burst.[6]

Of particular importance (for the lofted mass characteristics of the nuclear cloud) is the *particle size distribution* of the incipient ejecta mass. This size distribution is *not* provided by current cratering calculations. Physically, the particle size distribution will depend on, at least, the stress, strain, and temperature history of each element of the incipient ejecta. In general, as the ejecta flow into the air, the particle size distribution will vary with both the time of ejection and the range from the burst point. The incipient ejecta initially consist of vaporous soil and bomb debris material. At somewhat later times, melted soil flows into the fireball. The bulk of the ejecta, however, is composed of solid material which has been shocked to some peak pressure, distorted, and flowed by the cratering dynamics. For example, about 500 kton of soil experiences 7 kbar (100 ksi) or more of pressure in a 1 Mt yield surface burst. Thus, the crater ejecta particle size uncertainty involves not only natural in-situ size variations, but also uncertainties in soil/rock break-up and agglomeration during crater formation.

The crater does not completely form until about 5 seconds for a 1 Mt surface burst (an example of a predicted final crater profile is shown with a dashed line on Figure 5). Roughly 2 Mtons of ejecta mass (1 Mton = 10^{12} gm) is thrown from the crater, however, note that only a small fraction* of the ejecta mass becomes lofted as part of the nuclear cloud. Most of the mass falls back to earth between 10 seconds and 1 minute.

---

*It is estimated that ~0.3 Mtons of ejecta mass per Mt of weapon yield remains aloft at 5 minutes after detonation of a contact surface burst.

2.2 SWEEP-UP MASS SOURCE

For non-cratering HOB* detonations, the dust/pebbles which become entrained in the nuclear cloud originate very near the ground surface (probably within a few centimeters or so). A "dusty" sweep-up layer is formed as this near-surface material mixes with the high velocity winds behind the air shock wave. The sweep-up layer is fairly persistent, and some of the dust/pebble particles in this layer are subsequently drawn up into the main cloud.

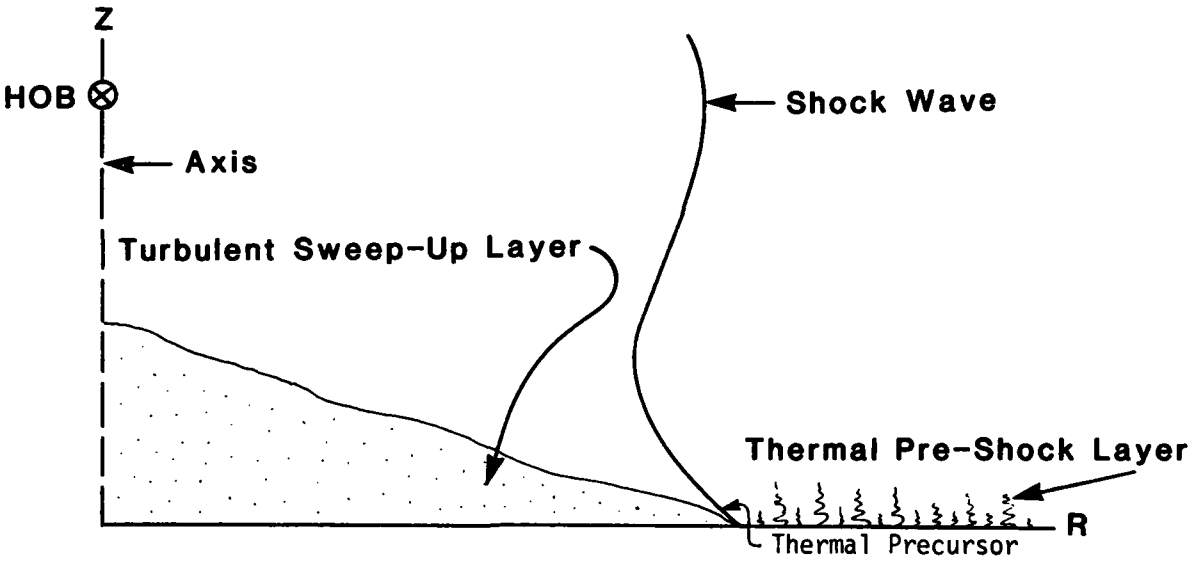

Thermal heating of an air layer near the ground surface may occur prior to shock arrival; this heated layer causes a thermal precursor flow field which appears to enhance the sweep-up layer. A thermal precursor is a pressure and velocity wave disturbance which travels faster in the heated near-surface thermal layer than in the cooler air above the surface.

---

*HOB is commonly used as an abbreviation for "height of burst" as well as the burst distance above the ground surface.

Figure 7 is a photographic example of a relatively late-time (~4 sec) sweep-up layer for shot GRABLE (W = 15 kt, HOB = 524 ft, SHOB = 212 ft/kt$^{1/3}$). Based on existing Nevada Test Site (NTS) data for SHOB between 150-500 ft/kt$^{1/3}$, the maximum radial extent of the sweep-up layer is about R_{max} ~1000-1300 ft/kt$^{1/3}$ which corresponds to a peak overpressure of ~5-10 psi. The maximum height of the sweep-up layer varies with the SHOB and ground surface characteristics, but a few hundred feet are typical for the relatively low yield NTS shots. Techniques for scaling the maximum radius and height of sweep-up layers to larger yields (say W ≧ 1 Mt) are still uncertain; however, estimates of ~1000 ft heights for W = 1 Mt seem plausible.

The early-time growth of the sweep-up layer is clearly coupled to the shock wave and air flow characteristics near the ground surface. Figure 8, drawn from photographs at 3 times after burst, illustrates the fact that the sweep-up layer begins forming very quickly behind the shock wave.

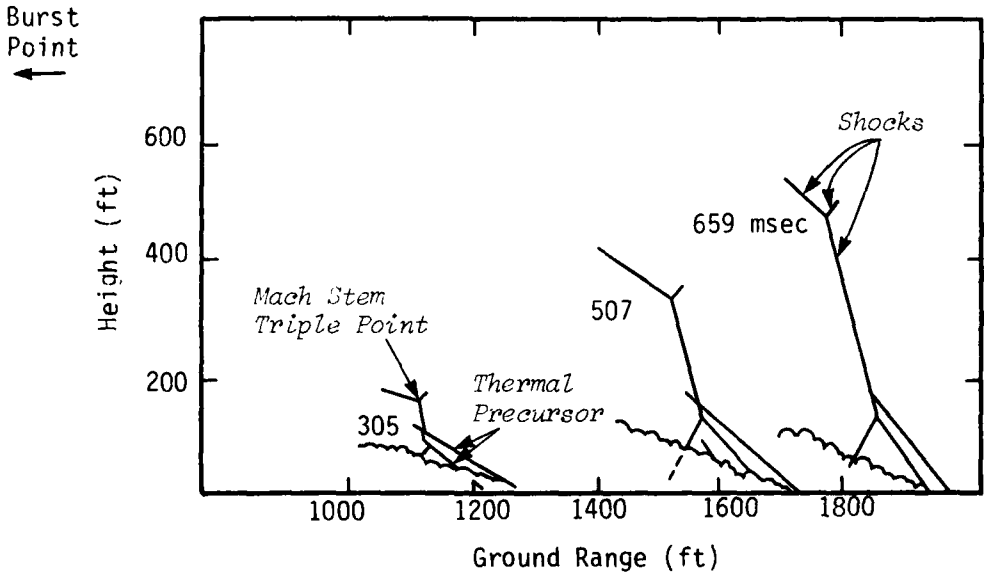

Fig. 8. Tracings from Technical Photography: Shot GRABLE.[7]

Fig. 7. Dusty Sweep-Up Layer for Shot GRABLE at t ~4-5 Seconds (W = 15 kt, HOB = 160 m).

The mass concentration or *density* (ρ) of the dust which becomes entrained in the sweep-up layer has been measured in two nuclear tests. For example, a density of about 2×10^{-3} gm/cm^3 has been measured in shot TEAPOT MET (W = 22 kt, SHOB = 140 ft/kt$^{1/3}$) at a range corresponding to peak overpressures and particle velocities of ~20 psi and ~600 ft/sec, respectively. This density was measured at a 3 ft height above the ground surface. Uncertainty factors of about 3 are suspected in this dust density measurement.

The actual concentration profile above the ground surface is not known; however, the following curve shows the general order of magnitude variation expected near the ground surface at a typical range and time in the sweep-up layer.

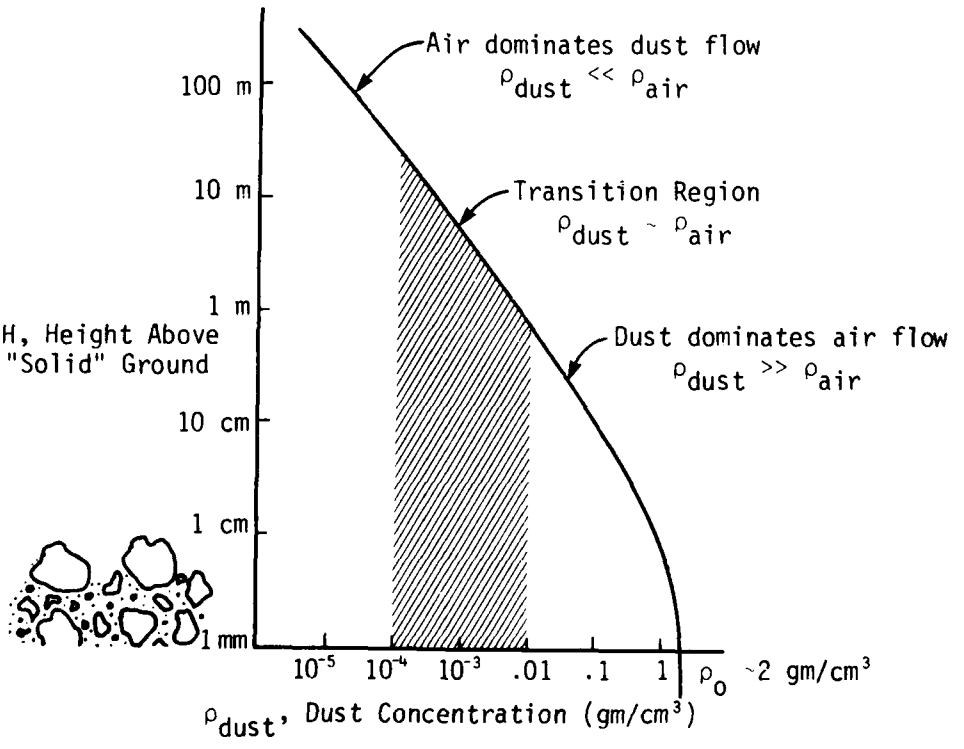

Fig. 9. Estimated Dust Concentration vs Height in the Sweep-Up Layer.

The high dust density region near the original ground surface represents the mass source for the sweep-up layer and ultimately the dust source for the nuclear cloud. The general nature of the interactions between the air and the near-surface material are sketched below:

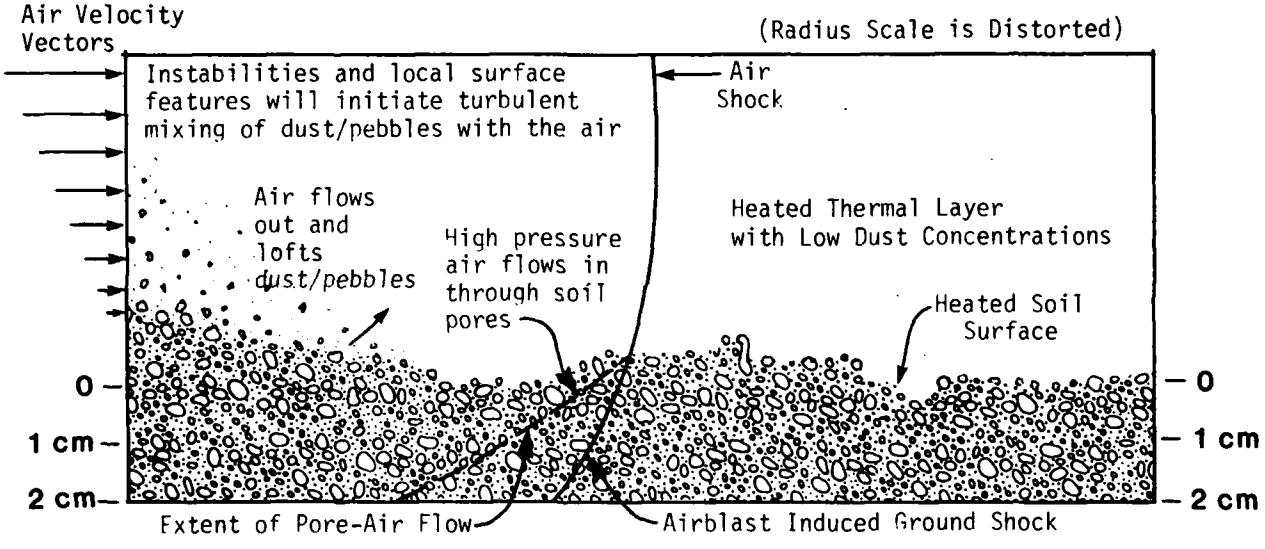

The multiphase physics (air plus solid/liquid soil particles) in the first 1-10 cm *above* and *below* the original ground surface involve viscous stresses which are associated with high gradients in horizontal air velocity near the ground surface. Also, the soil permeability and strength properties will determine the transfer of air momentum and energy to the near-surface soil material.

Immediately behind the shock wave on the ground, there will be some permeation (i.e., diffusion) of air into the porous surface material. The near-surface (~1 cm) permeability variations with depth and range will lead to scouring and lofting of near-surface material on a short-time scale. On a longer time scale, air will permeate through the pores deeper into the soil. As the overpressure on the surface subsequently decays, the air pressure in the pores below the surface will be higher for a time than the pressure being applied onto the surface by the decaying airblast wave. When the air pressures within the pores of the soil exceed the applied overpressure, there is an unbalanced upward force on material near the surface. Thus, soil material is ejected upward into the near-surface air flow and sweep-up layer. This effect has been observed in laboratory experiments and in HE field experiments, and has been theoretically calculated.

The deeper pore-air flow phenomenon may eject ~10 cm of soil material into the sweep-up layer.[8] There is probably a sufficient delay behind the shock wave that this material will not be accelerated to high velocities for a single burst. On the other hand, in a multiple nuclear burst environment, this phenomenon may represent the most significant dust/pebble/rock source for subsequent bursts at some sites. The permeability and cohesive strength of the shocked and heated ground material will probably be the most important site dependent physical characteristic for this phenomenon.

Once the dust/pebbles become lofted above a few meters, the complex air flow field behind the shock wave will dominate the further rise and turbulent diffusion of the dust/pebble mass.

The air flow field behind the near-surface shock wave is quite complicated due to

- unsteady pressure and flow dynamics including Mach stem and thermal precursor formation
- turbulent boundary layer effects involving in-situ bushes, trees, rocks/boulders, and small-scale hills/valleys

Many questions and issues remain unanswered in predicting the formation and nature of the sweep-up layer; Figure 10 summarizes some of these issues.

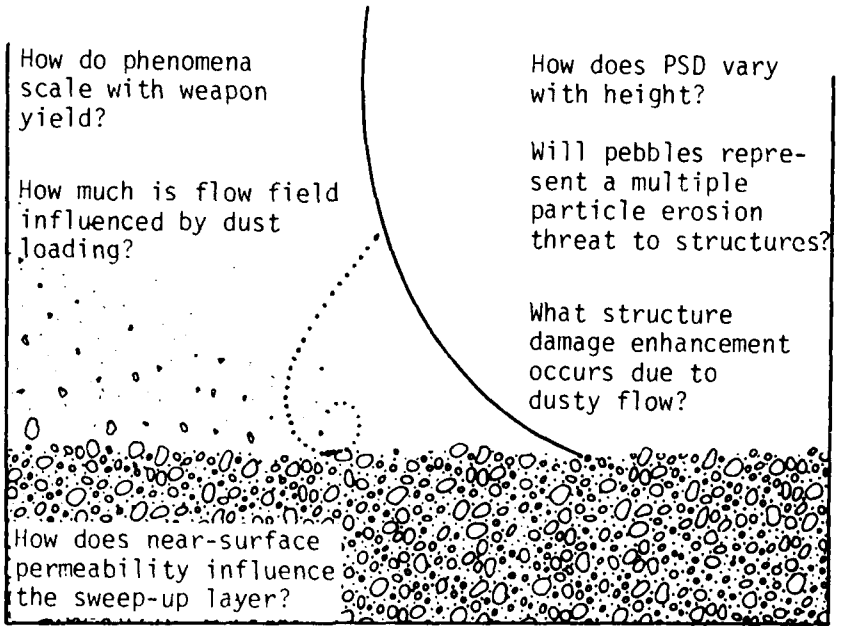

Fig. 10. Issues Concerning Sweep-Up Layer Dust and Pebbles.

SECTION 3

NUCLEAR CLOUD FORMATION

3.1 EARLY-TIME OR FIREBALL PHASE ($t \leq 10$ seconds for W = 1 Mt)

The very early-time phase ($t \leq 0.1$ second) of a nuclear cloud is characterized by extremely high fireball temperatures (10^5-10^6 °K) and shock wave pressures (10^3-10^6 psi) as indicated in the following Figures 11a and 11b. These curves are from a numerical simulation of a 2 Mt free air burst; this burst is equivalent to a 1 Mt contact surface burst over an idealized rigid surface with no crater and no ejecta.

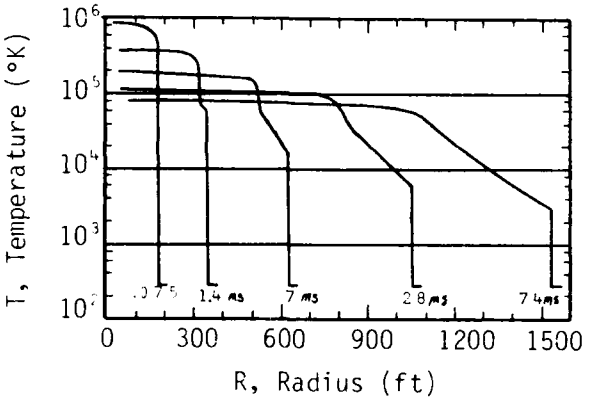

Fig. 11a. Fireball Temperature Versus Radius at Early Times in the Fireball History (1 Mt surface burst).[9]

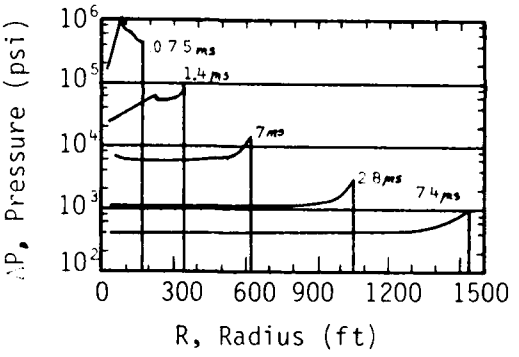

Fig. 11b. Overpressure Versus Radius at Early Times in the Fireball History (1 Mt Surface Burst).[9]

EXAMPLE:

At t = 28 milliseconds

R_{shock} 1,000 ft

T_{shock} 8,000°K

ΔP_{shock} 4,000 psi

At the fireball center (R = 0)

T ~100,000°K

ΔP ~1,000 psi

The late stages of the fireball growth and associated shock front behavior are indicated on Figures 11c to 11e. The persistence of the high fireball temperatures and low air densities (Figure 11d) set the stage for the *buoyancy dominated rise of the hot air* and the lofting of entrained dust/debris.

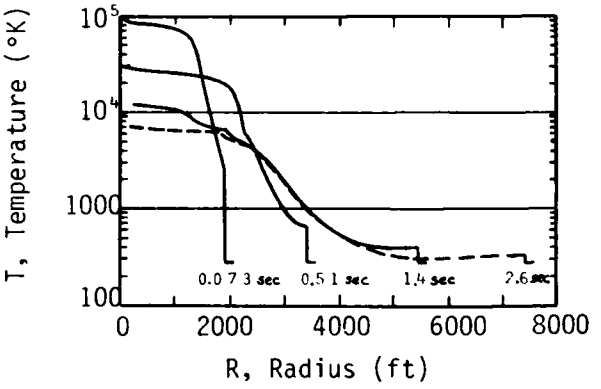

Fig. 11c. Late Fireball Temperature Versus Radius (1 Mt Surface Burst.)

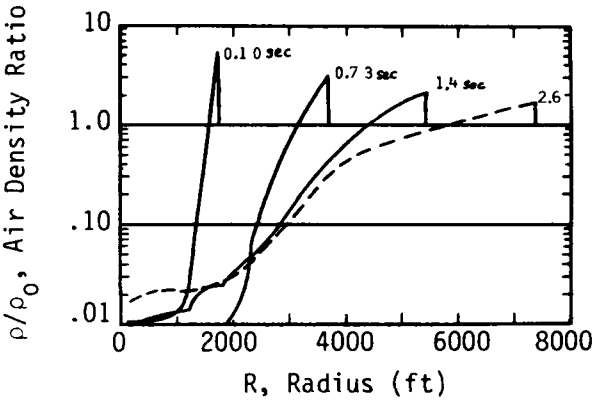

Fig. 11d. Late Fireball Density Ratios (ρ_0 ~1.2 x 10^{-3} gm/cm^3) Versus Radius (1 Mt Surface Burst).

Note that the results on Figures 11a to 11e are for an idealized 1-D spherical environment. The following two subsections indicate the effects on the early cloud of *crater ejecta* for contact surface bursts and the effects of *shock wave reflections* off the ground surface for HOB detonations.

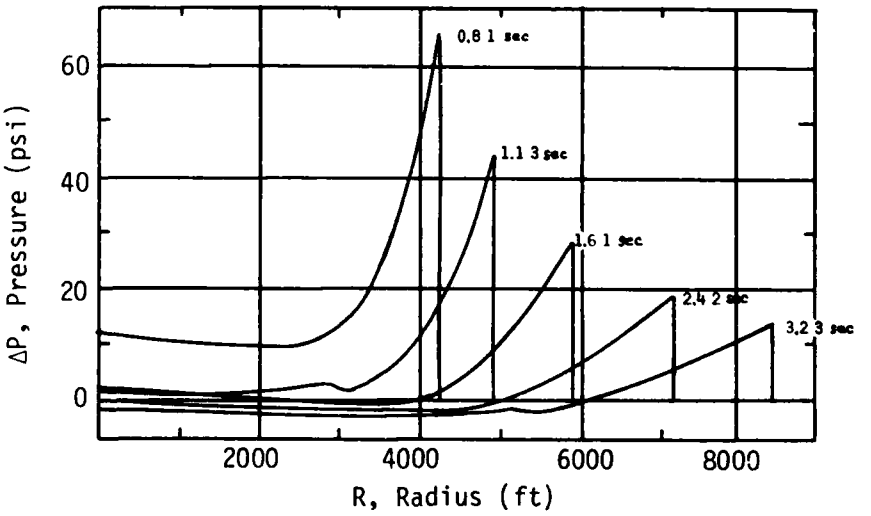

Fig. 11e. Overpressure Versus Radius (1 Mt Surface Burst).[9]

Early-Time Contact Surface Bursts

The detonation of a nuclear device very near the Earth's surface causes ground material to be thrown from the developing crater into the fireball. The initial pressures in the ground start at about 1000 Mbars (~1.5 x 10^{10} psi),[3] and consequently a strong shock wave develops and propagates into the local geologic material as described in Section 2.1. The geology is, therefore, quite important in determining the crater ejecta characteristics.

The ejecta flows into the fireball forming a dynamic multiphase region involving aerodynamic drag and thermal interactions. The thermal interactions include vaporization of solid/liquid material. The vaporization (and later recondensation) of the earth material is potentially significant when comparing shots on land with shots on water.

Figures 12a and 12b show predicted air velocities and temperatures 1 second after a 1 Mt contact surface burst on a soil/rock geology; estimated models were used for crater ejecta characteristics and multiphase drag/thermal interactions. Ejecta mass groups representing different size particles were assumed in the numerical calculations and each of these size groups will interact differently with the air. The boundaries of various size groups are shown on Figure 12a with the larger size particles traveling the larger distances from the burst point. The ejecta influences both the air velocities and temperatures. The temperatures (Figure 12b) are reduced in the interior of the fireball by relatively cold ejecta which mixes with the hotter air.

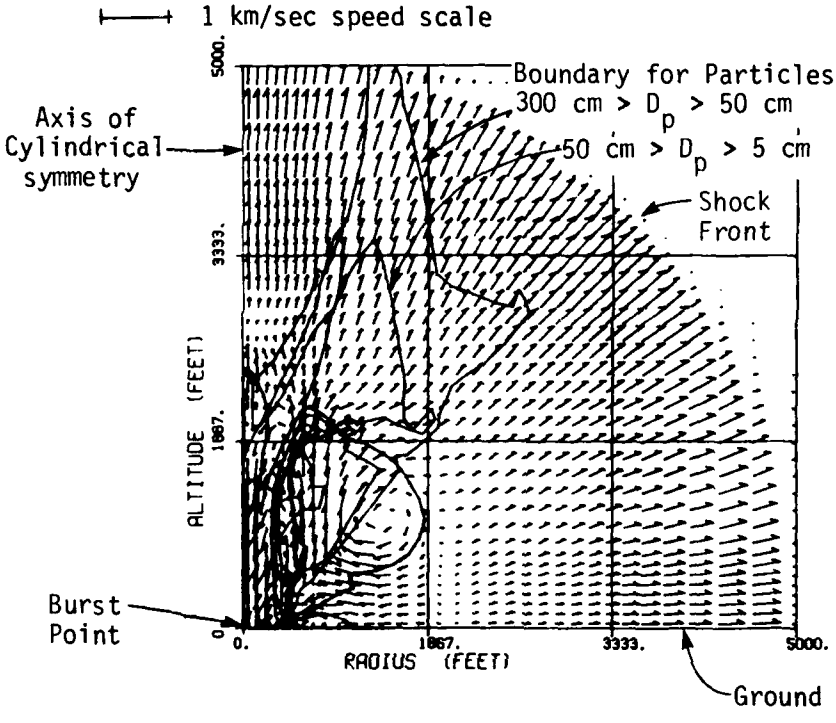

Velocity vectors show speed (use scale bar at top of figure) and direction of air mass near the base of each vector.

Fig. 12a. Air Velocity Field and Boundaries of Various Particle Size Groups for a 1 Mt Surface Burst at t = 1 sec.

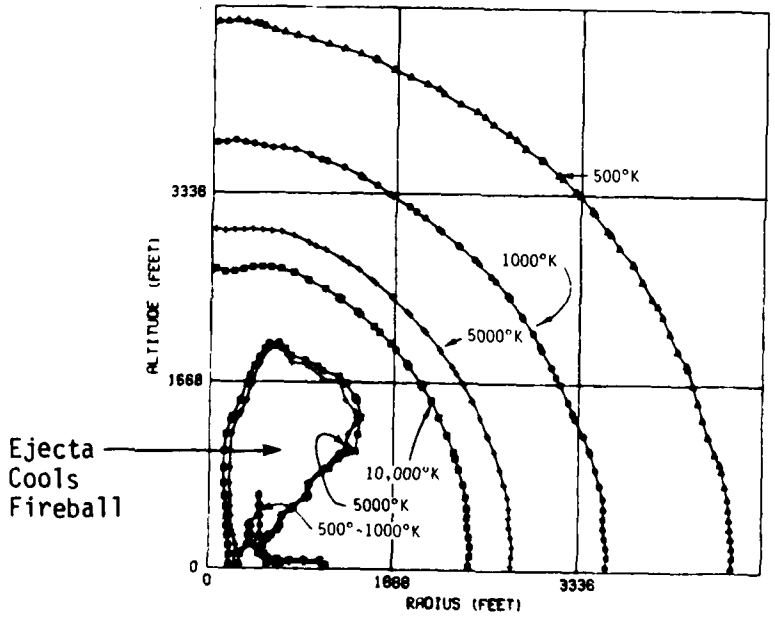

Fig. 12b. Air Temperature Field for a 1 Mt Surface Burst at t = 1 sec.[5]

The predicted dirt concentration field at t = 1 second is shown in Figure 12c. Concentrations of 10^{-2} gm/cm^3, which are ~10 times denser than ambient air, extend to altitudes of ~800 ft in this example. Concentrations of 10^{-6} gm/cm^3, which correspond to a relatively high concentration for natural water/ice clouds, extend to ~2000 ft in altitude. The mass at heights of ~3000 ft consists of the larger diameter particles which are not slowed down by aerodynamic drag.

Figure 12d shows the dirt concentration field at t = 14 seconds. The ejecta plume is near its maximum height of over 10,000 ft. The 10^{-6} gm/cm^3 contour extends to ~6000 ft. Buoyant lofting of the fireball and entrained particles has begun by this time.

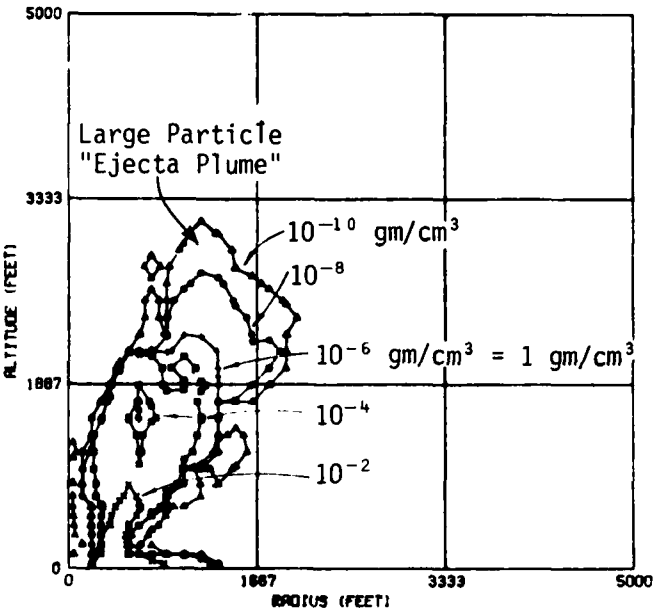

Fig. 12c. Lofted Soil/Rock Concentration Field for a 1 Mt Surface Burst at t = 1 sec.

(Note that radius and altitude scales have been increased by a factor of 3)

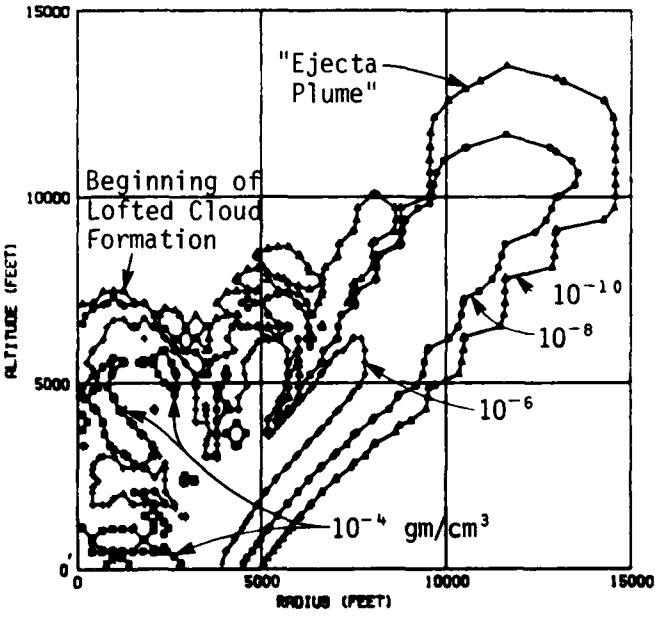

Fig. 12d. Lofted Soil/Rock Concentration Field for a 1 Mt Surface Burst at t = 14 sec.[5]

Early-Time HOB Detonations

As the height of the nuclear burst is increased above the Earth's surface, less of the weapon's energy is coupled to ground material and crater ejecta begins to play a smaller and smaller role in forming the nuclear cloud. This transitional region will not be discussed in detail; its characteristics are a combination of the contact surface burst phenomena discussed previously and the non-cratering HOB physical phenomena described in the remainder of this subsection.

When the spherical air shock wave from the burst interacts with the Earth's surface, complex reflected waves are transmitted back into the previously shocked air. These reflected waves strongly influence the subsequent flow field of the air and lofted material. Figures 13a and 13b show an example for shot U/K GRABLE (W = 15 kt, SHOB ~200 ft/kt$^{1/3}$) of predicted air velocity vectors just prior to and shortly after shock reflection off the ground.

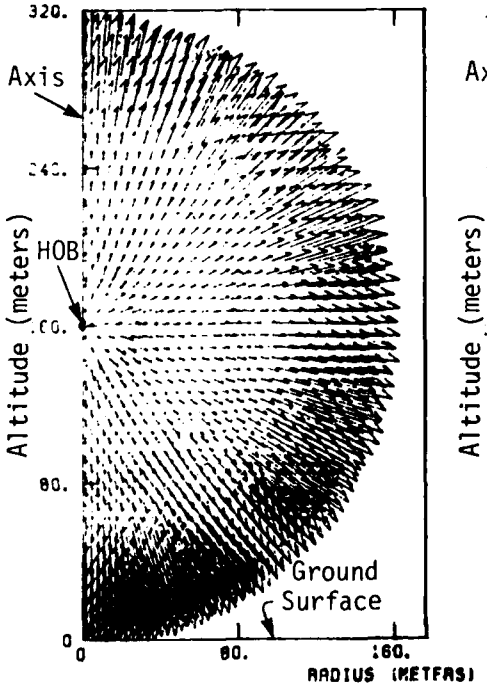

Fig. 13a. Velocity Field at t = 0.04 seconds for U/K GRABLE (W = 15 kt, HOB = 160 m).

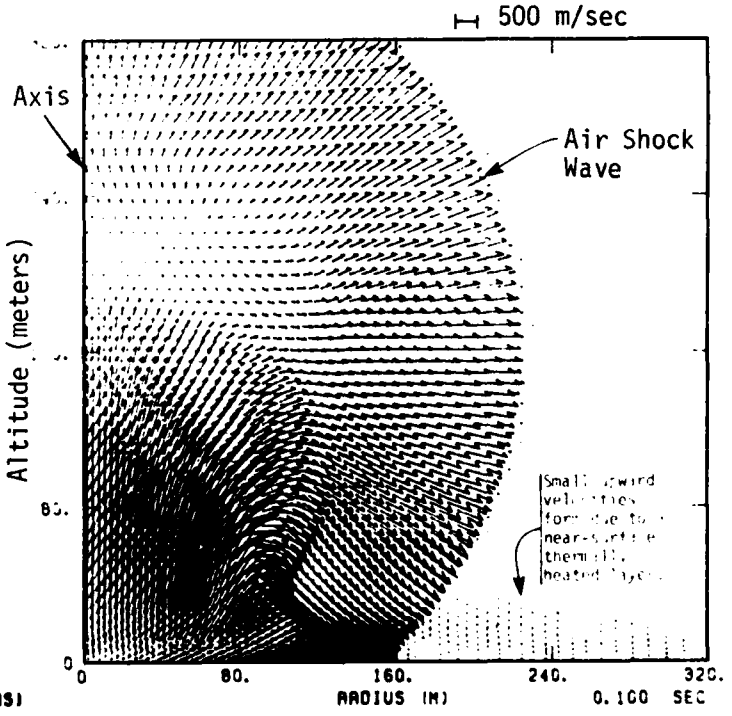

Fig. 13b. Velocity Field at t = 0.1 seconds for U/K GRABLE (W = 15 kt, HOB = 160 m).[10]

Figures 13c and 13d show the air flow fields at t = 0.3 and 0.5 seconds. During this time interval, the primary vortex or torus develops with its center at a radius of about 150 meters and a height of about 240 meters.

Downward directed winds develop above the ground surface and near the axis. A reversal point (RP) in velocity is identified on the adjacent figures. The relatively persistent downward flow will be eventually reversed by buoyancy forces; however, *the early entrainment of surface dust/pebbles into the rising fireball will be inhibited.*

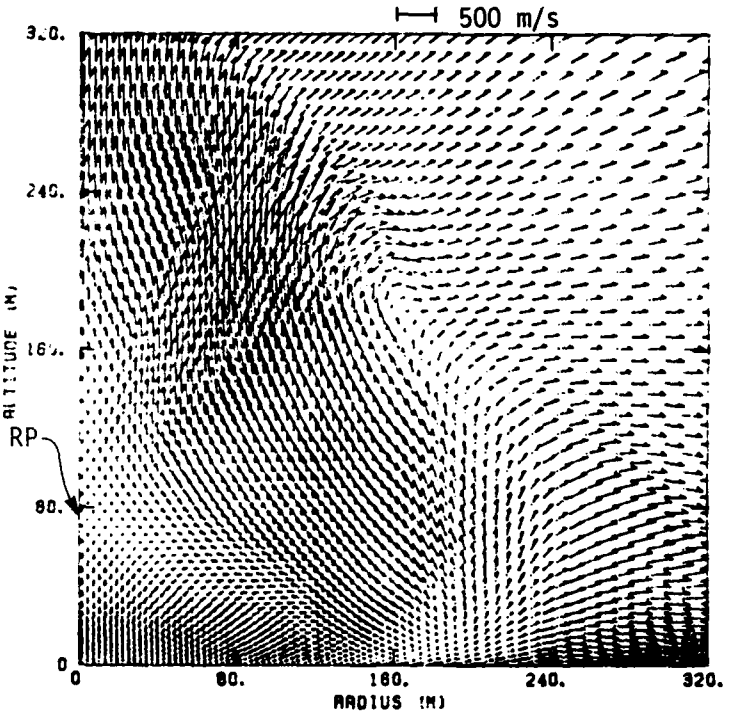

Fig. 13c. Velocity Field at t = 0.3 seconds for U/K GRABLE (W = 15 kt, HOB = 160 m).

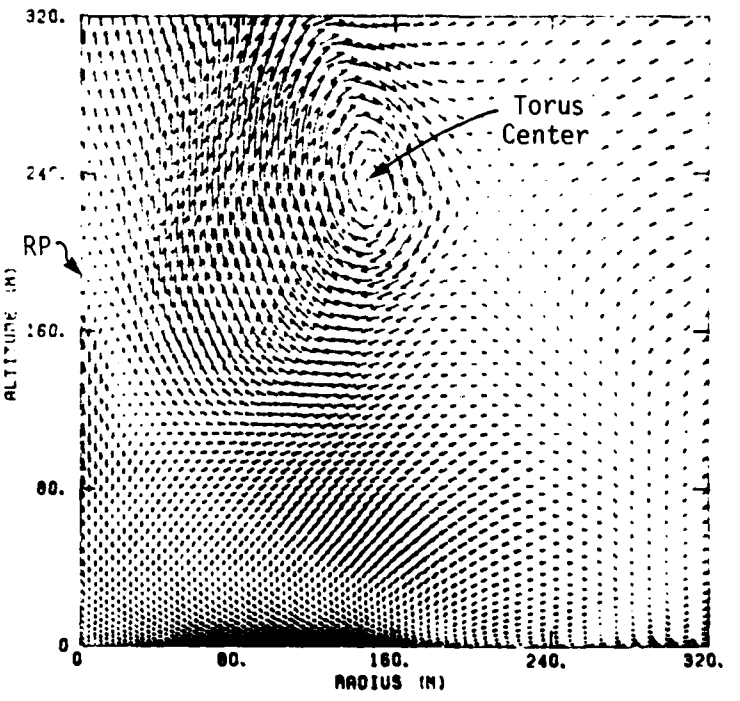

Fig. 13d. Velocity Field at t = 0.5 seconds for U/K GRABLE (W = 15 kt, HOB = 160 m).[10]

Figure 13e shows the predicted air velocity field and the visible fireball shape at t = 1.4 seconds for shot GRABLE. The theoretical/numerical predictions show that the upper fireball region and "tucked in" shape are associated with the torus flow field.

Also shown on Figure 13e is the estimated sweep-up layer height versus radius at this time. Note that the downward velocities below the reversal point (RP) are continuing to suppress the rise of the sweep-up mass near the axis.

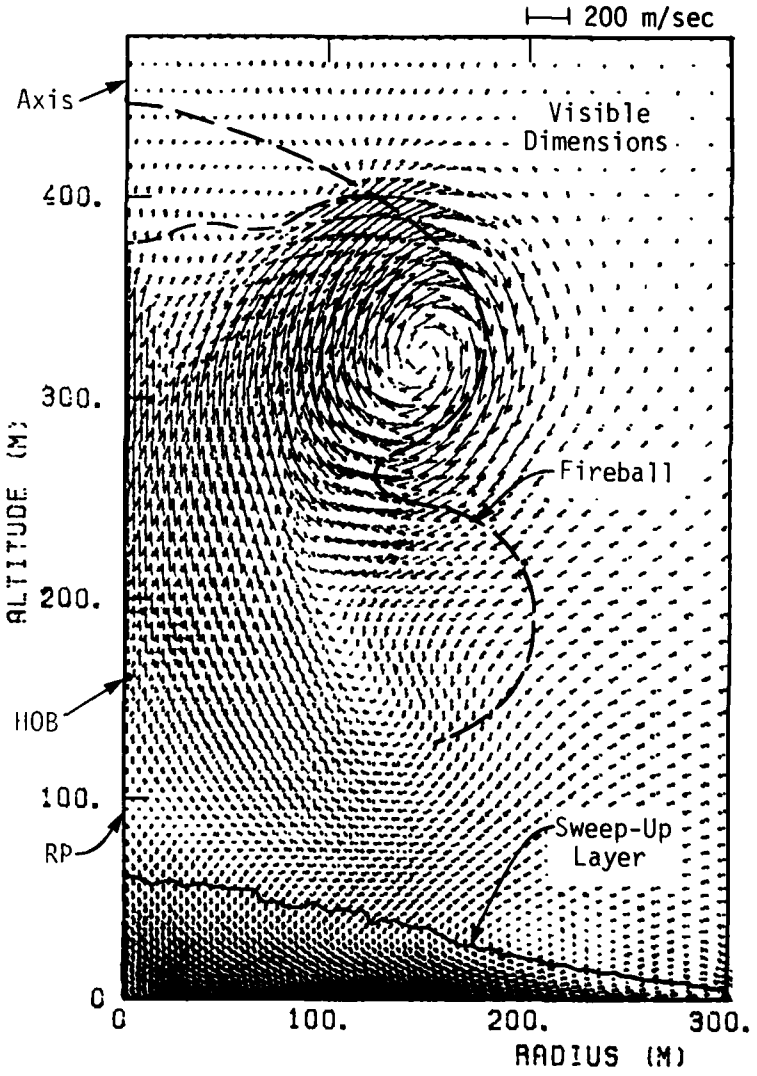

Fig. 13e. Velocity Field at t = 1.4 seconds for U/K GRABLE (W = 15 kt, HOB = 160 m).[10]

3.2 CLOUD RISE AND STABILIZATION PHASES (10 sec ≤ t ≤ 10 min)

After approximately 10-15 seconds for a 1 Mt burst, buoyancy forces begin to dominate the air velocity field characteristics. Buoyancy forces become important because the atmospheric pressure field returns to nearly ambient conditions, but peak air temperatures still exceed 1000°K at 10 seconds. The low density fireball air will accelerate upward causing a vortex air flow field to develop which entrains relatively cool air, earth material, radioactive material, and atmospheric humidity. The vortex flow carries the entrained material through the stem and into the upper portions of the cloud.

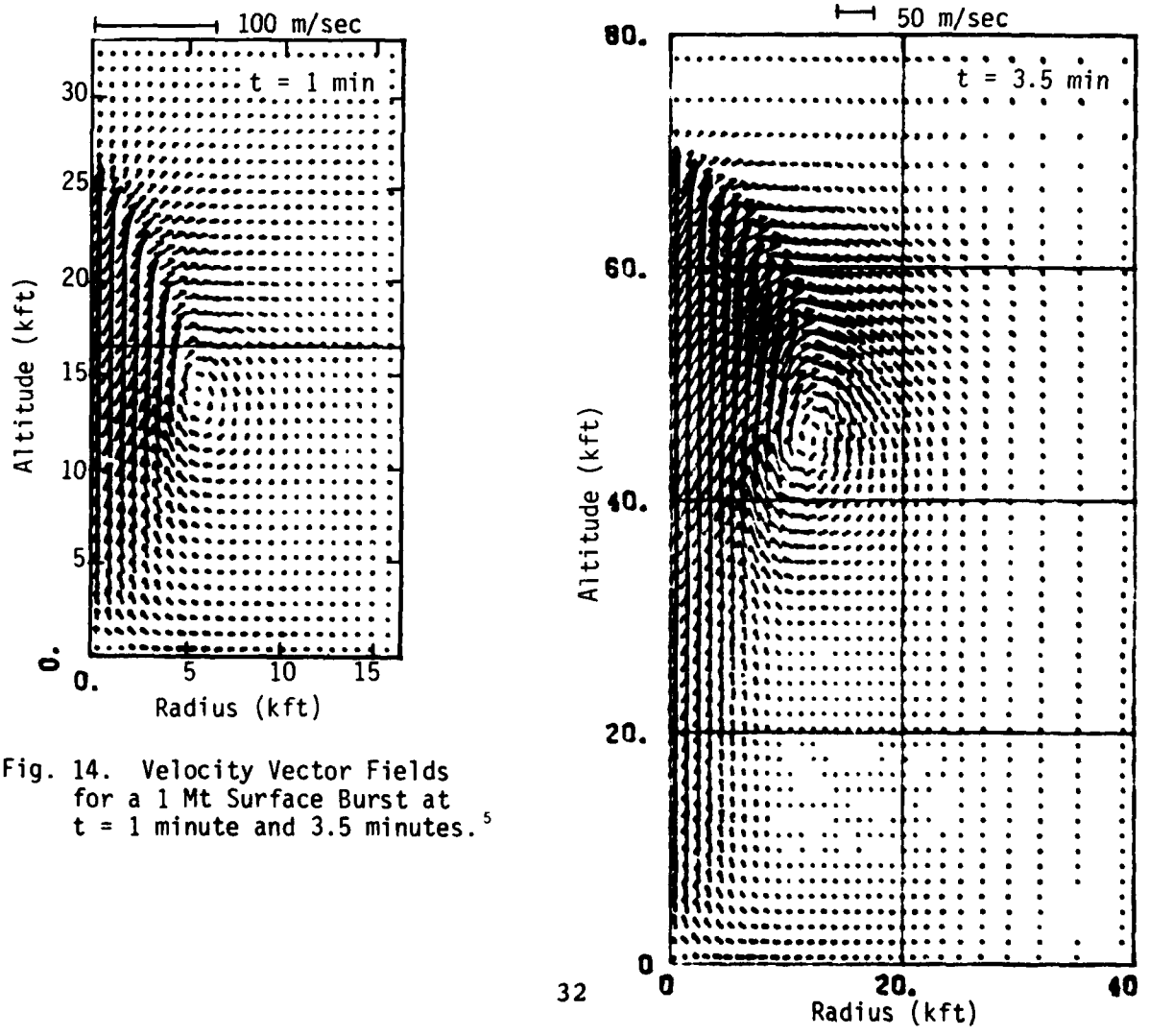

Fig. 14. Velocity Vector Fields for a 1 Mt Surface Burst at t = 1 minute and 3.5 minutes.[5]

At any time after burst, the amount of earth material and the spatial distribution of this material in the cloud depend on the weapon yield, HOB, and material properties (e.g., size distribution and strength) of the soil/rock. An example follows:

Figure 15 is an estimated spatial distribution of the lofted dust and pebble mass for a 1 Mt contact surface burst at 5 minutes after detonation. Figure 15a shows the mass concentration field. The altitude of the cloud is roughly 70,000 ft with a radius of approximately 20,000 ft at 5 minutes. Note that a vortex region of relatively high density (10^{-6} gm/cm^3) develops at an altitude of about 50,000 ft and a radius of between 10-15,000 ft.

The nature of the particle size distribution of this mass is presented in Figure 15b, which shows the cumulative lofted mass above any altitide Z at 5 minutes. Note that most of the mass is in the main cloud (about 210 kilotons of lofted mass above 40,000 ft); the stem contains about 50 kilotons of mass. The cumulative lofted mass is separated into "dust" mass (D_p < .5 cm) and "pebble" mass (.5 < D_p < .5 cm). At 5 minutes, over 40% of the lofted mass consists of pebbles. Most of the larger particles have landed on the ground by 5 minutes.

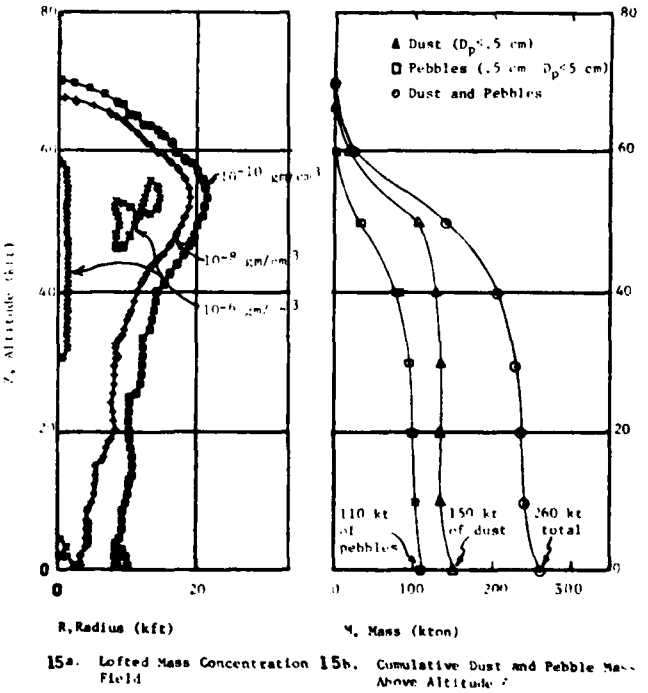

15a. Lofted Mass Concentration Field 15b. Cumulative Dust and Pebble Mass Above Altitude Z

Fig. 15. Lofted Dust/Pebble Spatial (R,Z) Distribution for a 1 Mt Surface Burst at 5 minutes.[5]

The buoyancy dominated phase ends when the cloud reaches its maximum or stabilized cloud altitude. This time is typically 3 to 5 minutes. While the cloud height will stop growing, and in fact decrease in many cases after a few minutes, the cloud diameter will continue to increase; the cloud diameter will increase until about 7-10 minutes even in the absence of atmospheric winds. The increase in cloud diameter is due to the post-stabilization air flow characteristics which occur near the cloud top as illustrated in Figure 16. The reverse vortex forms as a result of downflow of relatively dense air above the cloud top. Relatively dense air from lower altitudes is "pushed" upwards to lower density portions of the atmosphere; when the upward velocities caused by buoyancy get sufficiently small, gravitational forces on the relatively dense air dominate the flow field.

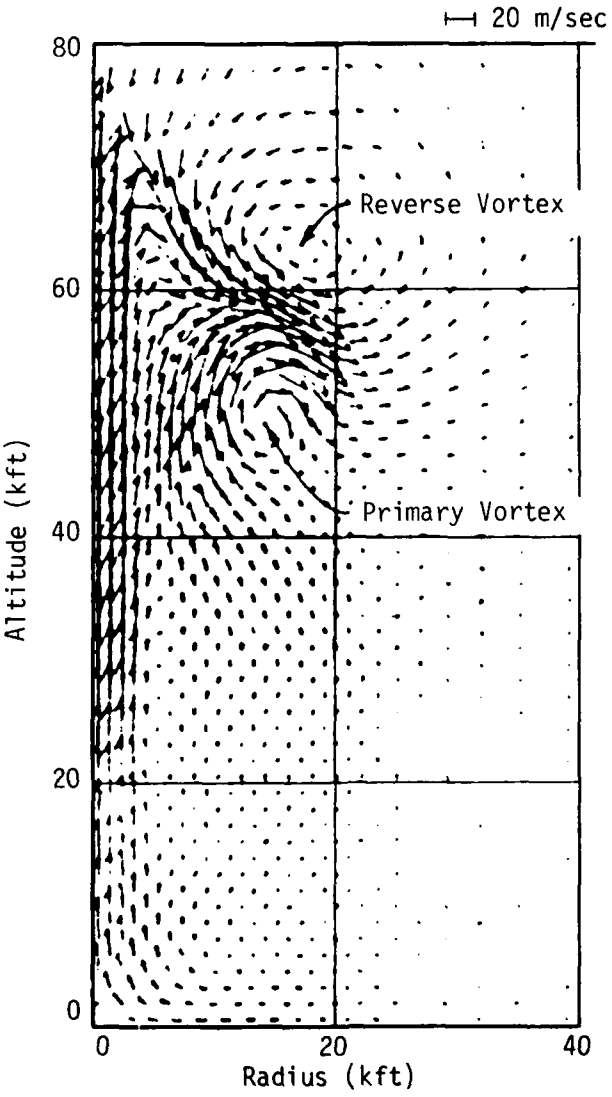

Fig. 16. Air Flow Field at 5 minutes for a 1 Mt Contact Surface Burst.[10]

3.3 EXPERIMENTAL CLOUD DIMENSION DATA

Figure 17 is an example of nuclear cloud dimensions versus time for shot CASTLE BRAVO (W = 15 Mt surface burst in the Pacific). At about 5 minutes, the cloud top reaches a maximum altitude of 114 kft; at 9 minutes, the cloud and stem diameter are about 330 kft and 28 kft, respectively.

Figure 18 shows experimental data for cloud altitude versus weapon yield at 1 minute after detonation; Figure 19 shows the maximum (or stabilized) cloud altitude versus yield. The various symbols on these figures indicate whether the shot was conducted in the Pacific or at the Nevada Test Site, and the type of measurement technique used. The scatter in the data is due primarily to variations in atmospheric conditions (e.g., winds, lapse rate, humidity) and/or measurement errors.

Figures 20 and 21 show experimental data for cloud diameter versus weapon yield at 1 minute and 10 minutes after detonation, respectively. Atmospheric winds and turbulence will often cause continued growth in the cloud diameter after 10 minutes.

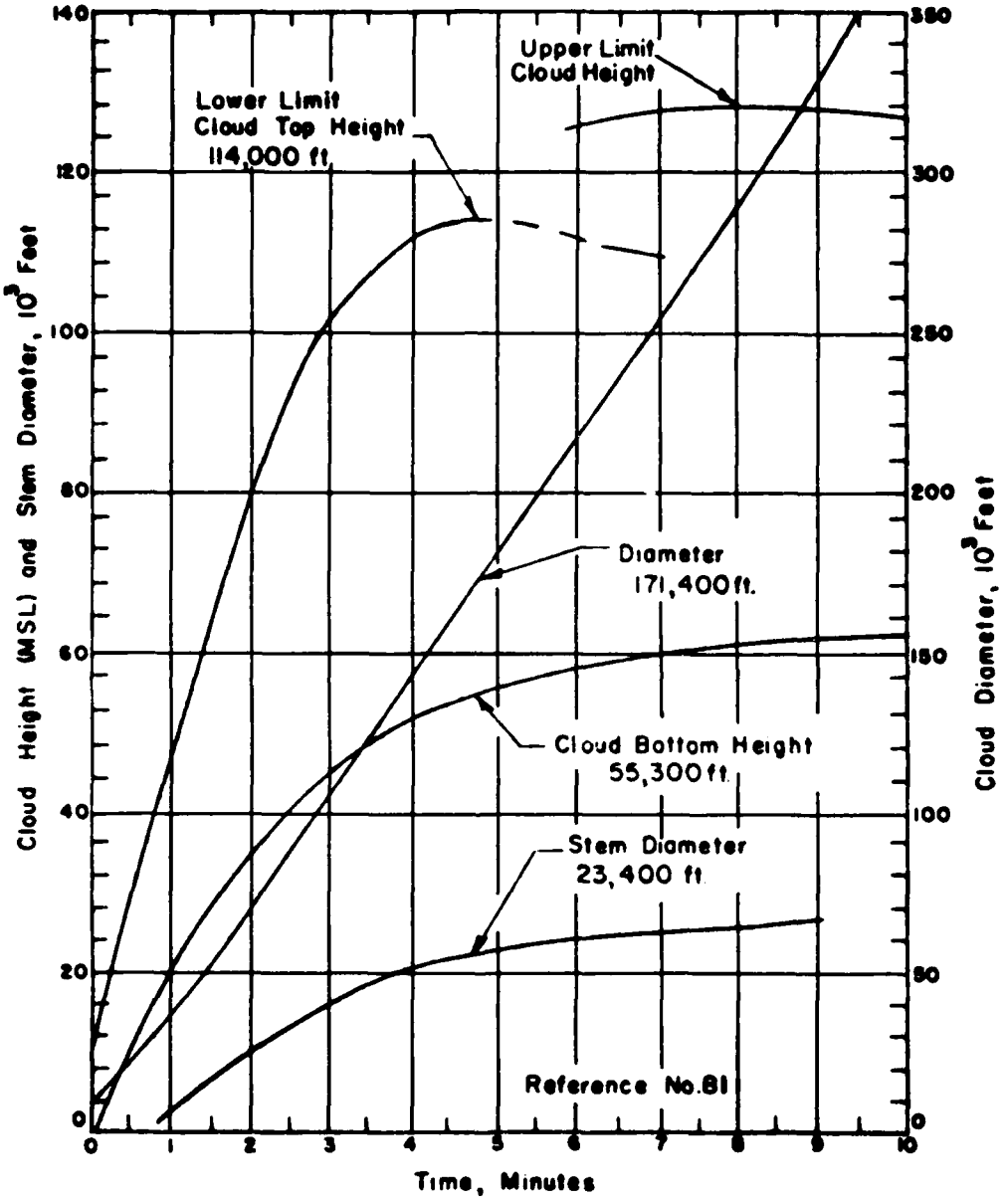

Fig. 17. Cloud Dimensions for Shot CASTLE BRAVO. (W = 15 Mt Surface Burst in the Pacific.)[11]

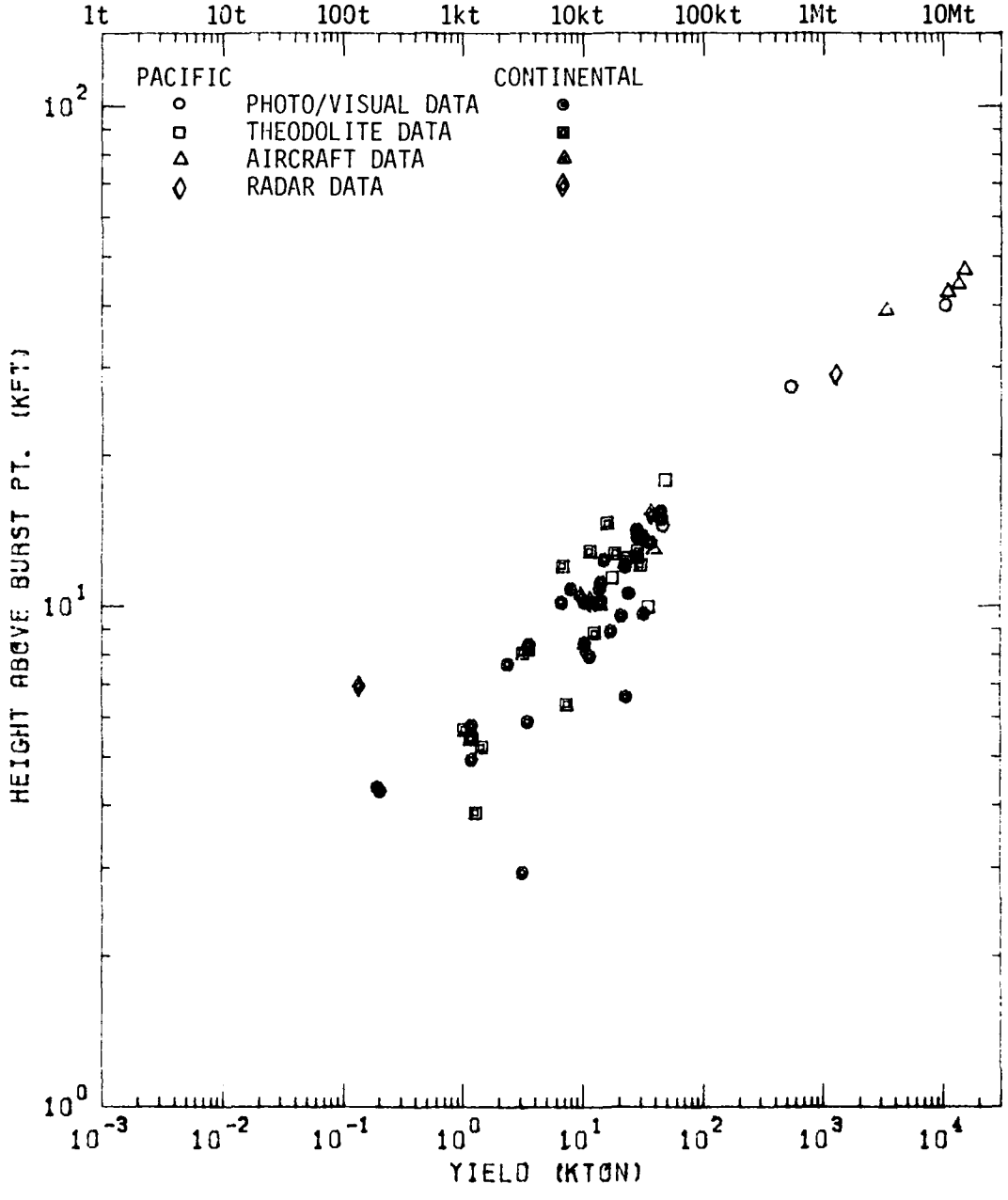

Fig. 18. Cloud Height Above Burst Point Versus Weapon Yield at t = 1 Minute.[1]

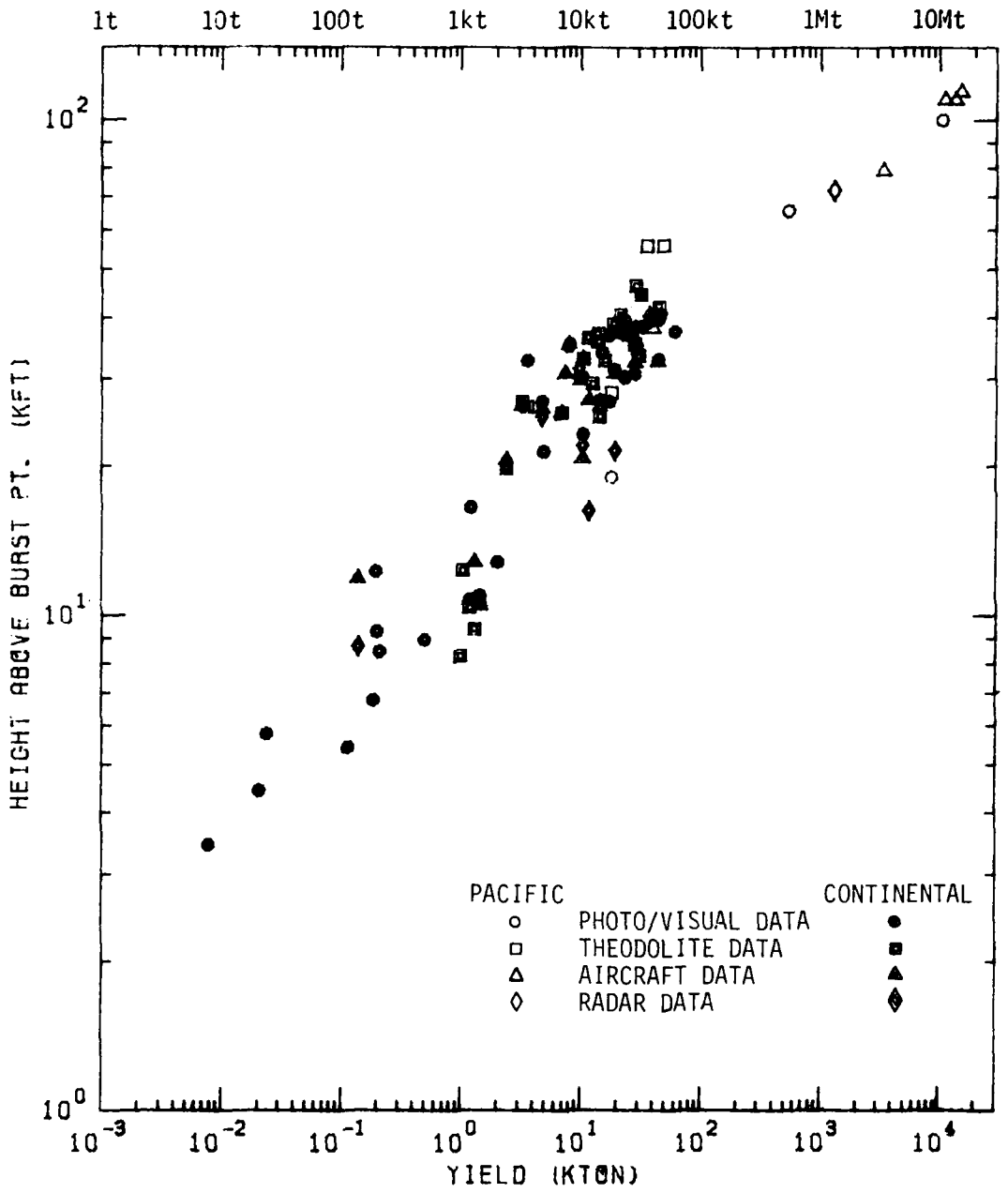

Fig. 19. Cloud Maximum/Stabilization Height Above Burst Point Versus Weapon Yield.[12]

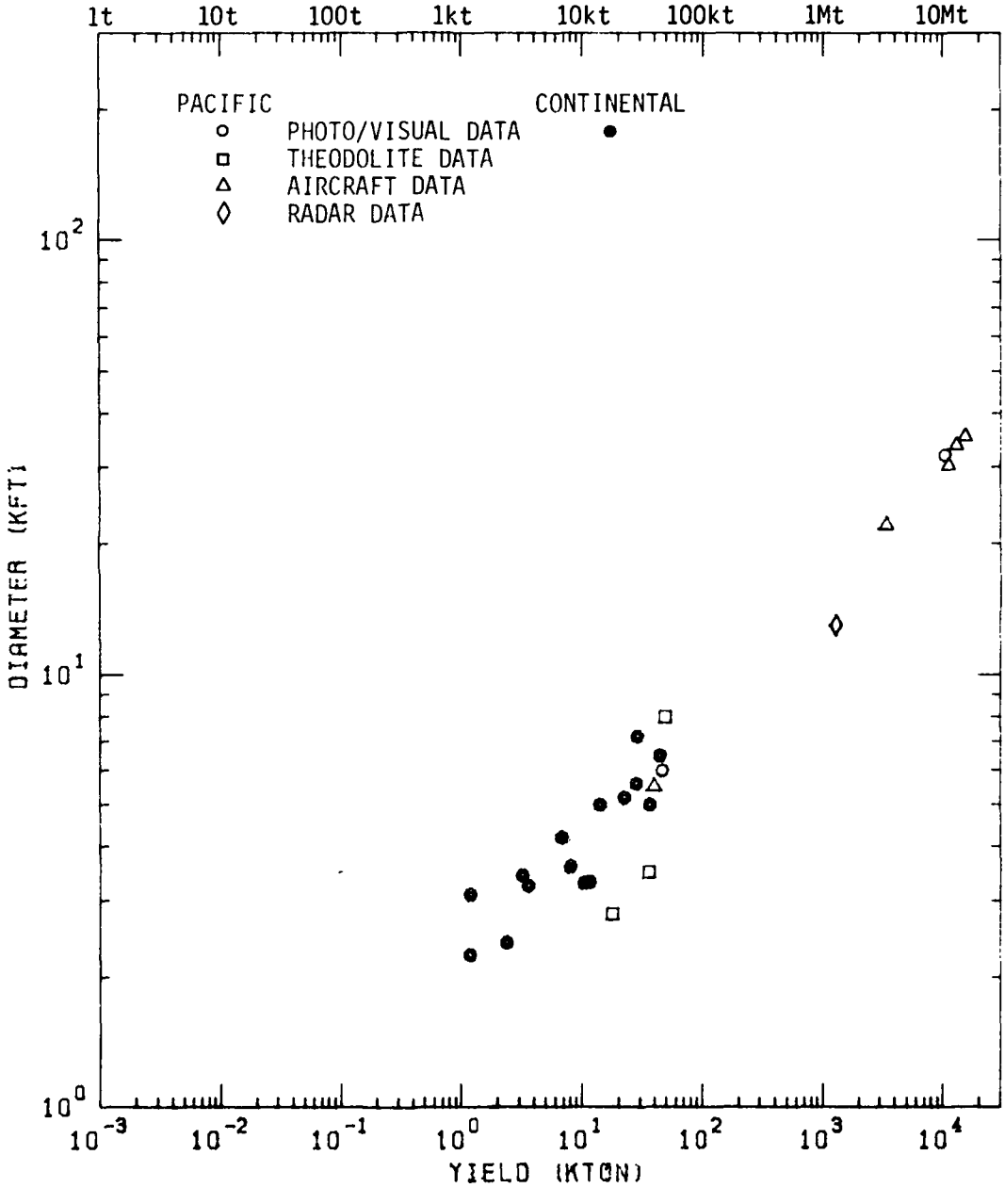

Fig. 20. Cloud Diameter Versus Weapon Yield at t = 1 Minute.[12]

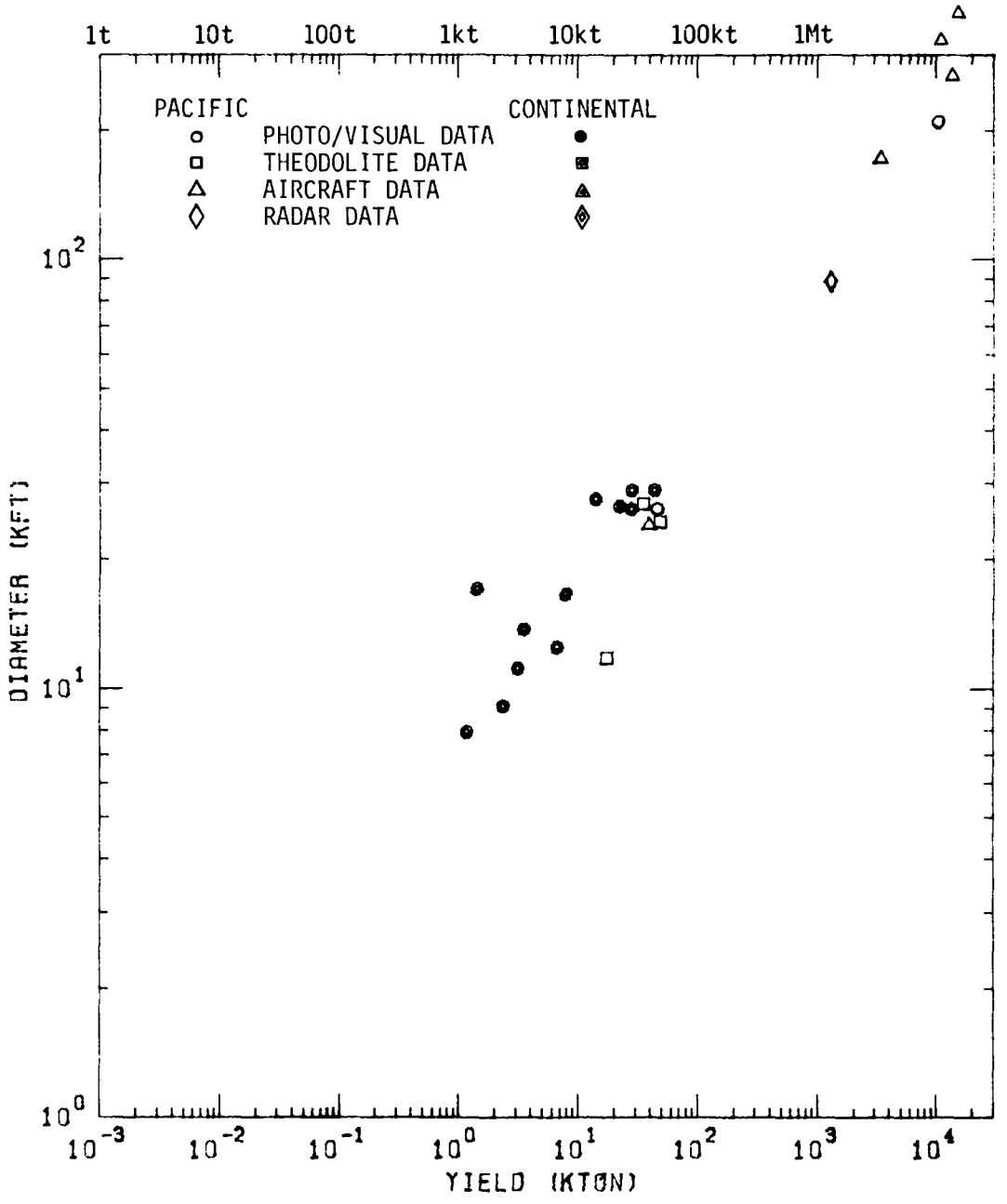

Fig. 21. Cloud Diameter Versus Weapon Yield at t = 10 Minutes.[12]

REFERENCES

1. S. Glasstone and P. J. Dolan (Eds.), The Effects of Nuclear Weapons, U.S. Department of Defense and U.S. Department of Energy, 1977.

2. J. E. Mansfield, W. M. Layson, R. T. Liner and J. T. Powers, Science Applications, Inc., Personal Communication, February 1975.

3. C. P. Knowles and H. L. Brode, "The Theory of Cratering Phenomena, An Overview", in Impact and Explosion Cratering, D. J. Roddy, R. O. Pepin and R. B. Merrill (Eds.), Pergamon Press, New York, 1977.

4. W. F. Dudziak and D. I. Devan, "Empirical SBM Data from Nuclear Detonation Photography", DNA 4132F, Information Science, Inc., September 1976.

5. M. Rosenblatt, G. Carpenter, G. E. Eggum, California Research & Technology, Inc., Unpublished Results, November 1978.

6. S. Schuster and K. N. Kreyenhagen, California Research & Technology, Inc., Personal Communication, April 1981.

7. W. E. Morris, J. Petes, E. R. Walthall and F. J. Oliver, Unpublished Results, August 1955.

8. L. Zernow, N. Louie, W. H. Andersen and P. J. Blatz, "An Experimental Study of the 'Reverse Percolation' Lofting Process in a Sand Medium", DNA 3210F, Shock Hydrodynamic, November 1973.

9. H. L. Brode, "Review of Nuclear Weapons Effects", Annual Review of Nuclear Science, Vol. 18, pg. 153, 1968.

10. M. Rosenblatt and R. S. Schlamp, "DICE Code Calculation of GRABLE (W = 15 kt, SHOB = 212 ft/kt$^{1/3}$) and Comparisons with Experimental Data", Presentation at DNA Nuclear Cloud Modeling Review Meeting, April 1981.

11. H. A. Hawthorne (Ed.), "Compilation of Local Fallout Data from Test Detonations 1945-1962 Extracted from DASA 1251, Volume II - Oceanic U.S. Tests", DNA 1251-2-EX, May 1979.

12. M. Rosenblatt, R. S. Schlamp and P. J. Hassig, California Research & Technology, Inc., Unpublished Results, November 1980.

DISTRIBUTION LIST

DEPARTMENT OF DEFENSE

Assistant to the Secretary of Defense
Atomic Energy
ATTN: Executive Assistant

Defense Communications Agency
ATTN: CCTC

Defense Intelligence Agency
ATTN: DT-2, T. Dorr
ATTN: DT-2
ATTN: DT-1C
ATTN: DB-4D

Defense Nuclear Agency
ATTN: NATA
ATTN: STSP
ATTN: SPSS
ATTN: SPTD
ATTN: STNA
3 cy ATTN: SPAS
4 cy ATTN: TITL

Defense Technical Information Center
12 cy ATTN: DD

Field Command
Defense Nuclear Agency
ATTN: FCPR, J. T. McDaniel
ATTN: FCTT
ATTN: FCTT, G. Ganong
ATTN: FCTXE
ATTN: FCTOF

Field Command
Defense Nuclear Agency
Livermore Branch
ATTN: FCPRL

Joint Chiefs of Staff
ATTN: J-5, Nuclear Division
ATTN: G050 (F-5 Force Plng & Prog Div)
ATTN: SAGA/SSD
ATTN: SAGA/SFD

Joint Strat Tgt Planning Staff
ATTN: JLA
ATTN: JPTM
ATTN: JPST
ATTN: JLTW-2

NATO School (SHAPE)
ATTN: U.S. Documents Officer

Under Secretary of Defense for Rsch & Engrg
ATTN: Strategic & Space Sys (OS)
ATTN: Engineering Technology, J. Persh

DEPARTMENT OF THE ARMY

BMD Advanced Technology Center
Department of the Army
ATTN: ATC-T, M. Capps

DEPARTMENT OF THE ARMY (Continued)

BMD Systems Command
Department of the Army
ATTN: BMDSC-H, N. Hurst

Deputy Chief of Staff for Ops & Plans
Department of the Army
ATTN: DAMO-NCZ

Deputy Chief of Staff for Rsch Dev & Acq
Department of the Army
ATTN: DAMA-CSS-N

Harry Diamond Laboratories
Department of the Army
ATTN: DELHD-NW-P (20240)
ATTN: DELHD-NW-P, J. Gwaltney (20240)
ATTN: DELHD-TF

U.S. Army Ballistic Research Labs
ATTN: DRDAR-BLV
ATTN: DRDAR-BLT, J. Frasier
ATTN: DRDAR-BL, R. Eichelberger
ATTN: DRDAR-BLV, W. Schuman, Jr
ATTN: DRDAR-BLT, R. Vitali
ATTN: DRDAR-BLT, J. Keefer

U.S. Army Material & Mechanics Rsch Ctr
ATTN: DRXMR-HH, J. Dignam

U.S. Army Materiel Dev & Readiness Cmd
ATTN: DRCDE-D, L. Flynn

U.S. Army Missile Command
ATTN: DRSMI-RH
ATTN: DRSMI-RKP, W. Thomas
ATTN: DRSMI-RHB, H. Greene

U.S. Army Nuclear & Chemical Agency
ATTN: Library

U.S. Army Research Office
ATTN: P. Radowski, Consultant

U.S. Army TRADOC Sys Analysis Actvy
ATTN: ATAA-TDC, R. Benson

DEPARTMENT OF THE NAVY

Naval Research Laboratory
ATTN: Code 2627
ATTN: Code 4773, G. Cooperstein
ATTN: Code 7908, A. Williams

Naval Sea Systems Command
ATTN: Sea-0352, M. Kinna

Naval Surface Weapons Center
White Oak Laboratory
ATTN: Code K06, C. Lyons
ATTN: Code F31
ATTN: Code R15, J. Petes

DEPARTMENT OF THE NAVY (Continued)

Naval Weapons Evaluation Facility
Kirtland Air Force Base
ATTN: P. Hughes
ATTN: Code 70, L. Oliver

Office of Naval Research
ATTN: Code 465

Office of the Chief of Naval Operations
ATTN: NOP 65
ATTN: OP 654C3, R. Piacesi
ATTN: OP 654E14

Strategic Systems Project Office
Department of the Navy
ATTN: NSP-272
ATTN: NSP-2722, F. Wimberly
ATTN: NSP-273

DEPARTMENT OF THE AIR FORCE

Aeronautical Systems Division
Air Force Systems Command
2 cy ATTN: ASD/ENFTV, D. Ward

Air Force Aeronautical Lab
ATTN: MBC, D. Schmidt
ATTN: LLM, T. Nicholas

Air Force Geophysics Laboratory
ATTN: LY, C. Touart

Air Force Rocket Propulsion Lab
ATTN: LKCP, G. Beale

Air Force Systems Command
ATTN: SOSS
ATTN: XRTO

Air Force Technical Applications Ctr
ATTN: TF

Air Force Weapons Laboratory
Air Force Systems Command
ATTN: SUL
ATTN: NTYV, A. Sharp
ATTN: DYV
ATTN: NTES
ATTN: HO, W. Minge
ATTN: DYV, E. Copus
2 cy ATTN: NTO

Air Force Wright Aeronautical Lab
ATTN: MLB, G. Schmitt

Air Force Wright Aernonautical Lab
ATTN: FIMG
ATTN: FBAC, D. Roselius

Air University Library
Department of the Air Force
ATTN: AUL-LSE

Arnold Engrg Dev Ctr
Department of the Air Force
ATTN: AEDC, DOFOV

DEPARTMENT OF THE AIR FORCE (Continued)

Ballistic Missile Office/DAA
Air Force Systems Command
ATTN: HQ Space Div/RST
ATTN: EN
ATTN: HQ Space Div/RSS
ATTN: ENSN, Blankinship
ATTN: ENMR
ATTN: SYDT
ATTN: ENSN, J. Allen

Deputy Chief of Staff
Research, Development, & Acq
Department of the Air Force
ATTN: AFRD
ATTN: AFRDQI

Foreign Technology Division
Air Force Systems Command
ATTN: SDBG
ATTN: TQTD
ATTN: SDBS, J. Pumphrey

Headquarters U.S. Air Force
ATTN: AFXOOTS

Space Division/YL
Department of the Air Force
ATTN: AFML

Strategic Air Command
Department of the Air Force
ATTN: XPQM
ATTN: DOXT
ATTN: XOBM
ATTN: XPFS

DEPARTMENT OF ENERGY

Department of Energy
ATTN: OMA/RD&T

OTHER GOVERNMENT AGENCY

Central Intelligence Agency
ATTN: OSWR/NED

DEPARTMENT OF ENERGY CONTRACTORS

Lawrence Livermore National Lab
ATTN: L-125, J. Keller
ATTN: L-8, R. Andrews
ATTN: L-262, J. Knox

Los Alamos National Laboratory
ATTN: R. S. Thurston
ATTN: MS670, J. McQueen
ATTN: R. W. Selden
ATTN: D. M. Kerr
ATTN: R. S. Dingus
ATTN: J. C. Hopkins

Sandia National Laboratories
Livermore Laboratory
ATTN: T. Cook
ATTN: Library & Security Classification Div
ATTN: H. Norris

DEPARTMENT OF ENERGY CONTRACTORS (Continued)

Sandia National Lab
ATTN: M. Cowan
ATTN: A. Chabai

DEPARTMENT OF DEFENSE CONTRACTORS

Acurex Corp
ATTN: R. Rindal
ATTN: C. Powars
ATTN: C. Nardo

Aerojet Solid Propulsion Co
ATTN: R. Steele

Aerospace Corp
ATTN: H. Blaes
ATTN: W. Barry
ATTN: R. Crolius

Analytic Services, Inc
ATTN: J. Selig

Aptek, Inc
ATTN: T. Meagher

Avco Research & Systems Group
ATTN: W. Broding
ATTN: J. Gilmore
ATTN: Document Control
ATTN: J. Stevens
ATTN: A. Pallone
ATTN: W. Reinecke
ATTN: P. Grady

Battelle Memorial Institute
ATTN: M. Vanderlind
ATTN: E. Unger
ATTN: R. Castle

Boeing Co
ATTN: R. Holmes
ATTN: M/S 85/20, E. York
ATTN: B. Lempriere
ATTN: R. Dyrdahl

California Research & Technology, Inc
4 cy ATTN: M. Rosenblatt
ATTN: K. Kreyenhagen

Calspan Corp
ATTN: M. Holden

Clark University
ATTN: D. Sachs

Dupont Chemical Corp
ATTN: F. Bailey

Effects Technology, Inc
ATTN: R. Parisse

General Electric Co
ATTN: P. Cline
ATTN: B. Maguire

General Research Corp
ATTN: J. Mate

DEPARTMENT OF DEFENSE CONTRACTORS (Continued)

H-Tech Labs, Inc
ATTN: B. Hartenbaum

Harold Rosenbaum Associates, Inc
ATTN: G. Weber

Hercules, Inc
ATTN: P. McAllister

Institute for Defense Analyses
ATTN: Classified Library

Kaman Sciences Corp
ATTN: J. Harper
ATTN: J. Hoffman
ATTN: J. Keith
ATTN: F. Shelton

Kaman Sciences Corp
ATTN: D. Sachs

Kaman Tempo
ATTN: DASIAC
ATTN: B. Gambill

Lockheed Missiles & Space Co, Inc
ATTN: F. Borgardt

Lockheed Missiles & Space Co, Inc
ATTN: R. Walz

Los Alamos Technical Associates, Inc
ATTN: P. Hughes

Martin Marietta Corp
ATTN: E. Strauss

McDonnell Douglas Corp
ATTN: E. Fitzgerald
ATTN: H. Hurwicz
ATTN: L. Cohen
ATTN: G. Johnson
ATTN: J. Garibotti
ATTN: H. Berkowitz
ATTN: P. Lewis, Jr
ATTN: D. Dean
ATTN: R. Reck

McDonnell Douglas Corp
ATTN: M. Potter

National Academy of Sciences
ATTN: National Materials Advisory Board
ATTN: D. Groves

Pacific-Sierra Research Corp
ATTN: G. Lang
ATTN: H. Brode

Pan Am World Service Inc
ATTN: AEDC/Library Doc (TRF)

Physics International Co
ATTN: J. Shea

DEPARTMENT OF DEFENSE CONTRACTORS (Continued)

PDA Engineering
ATTN: J. Dunn
ATTN: J. McDonald
ATTN: M. Sherman

R & D Associates
ATTN: A. Field
ATTN: J. Carpenter
ATTN: P. Rausch
ATTN: W. Graham
ATTN: P. Haas

Rand Corp
ATTN: R. Rapp

Rockwell International Corp
ATTN: B. Schulkin
ATTN: G. Perroue

Science Applications, Inc
ATTN: J. Manship
ATTN: W. Yengst
ATTN: J. Warner
ATTN: W. Plows
ATTN: C. Lee
ATTN: J. Stoddard

Science Applications, Inc
ATTN: W. Layson
ATTN: J. Cockayne

Science Applications, Inc
ATTN: A. Martellucci

Science Applications, Inc
ATTN: J. Burghart

Southern Research Institute
ATTN: C. Pears

SRI International
ATTN: P. Dolan
ATTN: G. Abrahamson
ATTN: D. Curran
ATTN: H. Lindberg

DEPARTMENT OF DEFENSE CONTRACTORS (Continued)

System Planning Corp
ATTN: J. Jones

Systems, Science & Software, Inc
ATTN: G. Gurtman
ATTN: R. Duff

Terra Tek, Inc
ATTN: S. Green

Thiokol Corp
ATTN: W. Shoun
ATTN: J. Hinchman

TRW Defense & Space Sys Group
ATTN: M. Seizew
ATTN: N. Lipner
ATTN: R. Bacharach
ATTN: T. Williams
ATTN: P. Brandt
ATTN: G. Arenguren
ATTN: D. Baer
ATTN: W. Wood
ATTN: A. Zimmerman
ATTN: A. Ambrosio
ATTN: T. Mazzola
ATTN: M. King
ATTN: R. Plebuch
2 cy ATTN: I. Alber

TRW Defense & Space Sys Group
ATTN: P. Dai
ATTN: W. Polich
ATTN: E. Wong
ATTN: D. Kennedy
ATTN: D. Glenn
ATTN: L. Berger
ATTN: E. Allen
ATTN: N. Guiles
ATTN: V. Blankinship

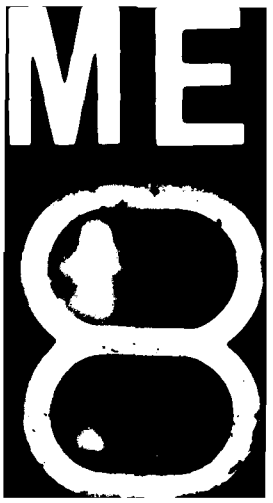
ME
80